Open access • Posted Content • DOI:10.1101/2021.09.23.461562

Chronic THC vapor rescues inflammation-related thermal hyperalgesia and causes cell type-specific modifications in vlPAG neurons — Source link

Leslie K Kelley, Jason W. Middleton, Nicholas W. Gilpin, S. H. Lightfoot ...+1 more authors

Institutions: LSU Health Sciences Center New Orleans, University of Calgary

Published on: 24 Sep 2021 - bioRxiv (Cold Spring Harbor Laboratory)

Topics: Chronic pain, Opioid, Cannabinoid and Periaqueductal gray

Chronic THC vapor rescues inflammation-related thermal hyperalgesia and causes cell type-specific modifications in vlPAG neurons

Abbreviated Title: THC vapor inhalation modulates pain and midbrain neural circuits

Authors: Leslie K. Kelley[1,2], Savannah H.M. Lightfoot[3], Matthew N. Hill[3], *Nicholas W. Gilpin[1,2,4,5], *Jason W. Middleton[2,4,5,6]

Departments of [1]Physiology, and [6]Cell Biology and Anatomy, Louisiana State University Health Sciences Center, New Orleans, LA 70112

[2]Alcohol and Drug of Abuse Center of Excellence, LSUHSC, New Orleans, LA

[3]Hotchkiss Brain Institute, Departments of Cell Biology and Anatomy & Psychiatry, University of Calgary, Calgary, AB, Canada T2N 4N1

[4]Neuroscience Center of Excellence, Louisiana State University Health Science Center, New Orleans, LA 70112

[5]Southeast Louisiana VA Healthcare System, New Orleans, LA

*Co-corresponding authors: jmidd3@lsuhsc.edu, ngilpi@lsuhsc.edu

Abstract

To reduce reliance on opioids for the treatment of pain in the clinic, ongoing work is testing the utility of cannabinoid drugs as a potential alternative for treatment of chronic pain and/or as a strategy for reducing opioid drug dosage and duration of treatment (i.e., so-called opioid-sparing effects). Previous preclinical work has shown robust anti-hyperalgesic effects of systemic THC and acute anti-hyperalgesic effects of vaporized THC. Here, we used a vapor inhalation model in rats to test chronic THC vapor inhalation effects on thermal nociception and mechanical sensitivity, as well as midbrain (i.e., periaqueductal gray [PAG]) neuronal function, in adult male rats with chronic inflammatory pain. We report that chronic THC vapor inhalation produces a robust anti-hyperalgesic effect in rats with chronic inflammatory pain, and that this effect persists 24 hours after cessation of THC exposure. We demonstrate that chronic THC vapor inhalation also modulates intrinsic and synaptic properties of ventrolateral PAG (vlPAG) neurons, including reductions in action potential firing rate and reductions in spontaneous inhibitory synaptic transmission, and that these effects occur specifically in neurons that respond to current input with a delayed firing phenotype. Finally, we show that the suppressive effect of the bath-applied mu-opioid receptor (MOR) agonist DAMGO on synaptic inhibition in the vlPAG is enhanced in slices taken from rats with a history of chronic THC vapor inhalation. Collectively, these data show that chronic THC vapor inhalation produces lasting attenuation of thermal hyperalgesia and reduces synaptic inhibition in the vlPAG of rats with chronic inflammatory pain.

Significance Statement

Many adults in the U.S. with pain self-medicate with THC and cannabis, and many cannabis users are increasingly using e-cigarette type devices filled with cannabis extracts to self-administer THC and other constituents of the marijuana plant. Until recently, most rodent studies of THC effects on brain and behavior have not used vapor inhalation techniques. Here, we designed a series of studies to test the effect of chronic THC vapor inhalation on pain-related behaviors and midbrain neural circuit function in adult male Wistar rats. We hypothesized that chronic THC vapor would have anti-hyperalgesic effects in rats with chronic inflammatory pain, and that it would produce disinhibition of midbrain pain modulation neurons.

Introduction

Cannabinoids are a promising potential alternative to opioids for the treatment of chronic pain (Nielsen et al., 2017). Interestingly, chronic pain is the most common reason reported for using medicinal cannabis (Baron et al., 2018). With medicinal cannabis approved in 34 U.S. states and recreational cannabis approved in 12 U.S. states (13), many adults with pain self-medicate with THC and cannabis (Reiman et al., 2017; Sturgeon et al., 2020), and many cannabis users are increasingly using e-cigarette type devices filled with cannabis extracts to self-administer THC and other constituents of the marijuana plant (Morean et al., 2015; Mammen et al., 2016; Morean et al., 2017). Evidence collected in humans suggests that cannabis is analgesic and therefore may hold promise as a therapeutic substitute for opioids in the clinic (Boehnke et al., 2016; Bradford and Bradford, 2017; Cooper et al., 2018). There is a gap in the preclinical and clinical literature regarding THC vapor effects on the brain in individuals living with chronic pain, as well as ideal THC vapor delivery protocols for effectively reducing pain.

One promising strategy for reducing pain is via modulation of descending pain facilitation and inhibition circuits (Millan, 2002; Tracey and Mantyh, 2007). One potential point of intervention is at the level of the ventrolateral periaqueductal gray (vlPAG). Chronic inflammatory pain decreases tonic inhibitory current and increases spontaneous inhibitory postsynaptic current frequency in vlPAG neurons in female rats (Tonsfeldt et al., 2016) and increases action potential firing in phasic-firing vlPAG neurons in male and female rats (McPherson et al., 2021). Opioids reduce pain, in part,

via activation of descending vlPAG outputs to the rostral ventrolateral medulla (RVM) in adult male rats (Basbaum and Fields, 1984; Hirakawa et al., 1999). Activity of the vlPAG is upregulated by opioid receptor agonists in adult male rats (Loyd et al., 2007), and activation of mu-opioid receptors disinhibits vlPAG neurons through local GABAergic inputs in adult male mice (Li et al., 2016).

While the mechanisms underlying the anti-nociceptive effects of cannabinoids are not completely understood, it is known that cannabinoids reduce inflammation and modulate pain via actions in central pain pathways (Guindon and Hohmann, 2009; Woodhams et al., 2017). More specifically, cannabinoids are thought to reduce pain via activation of cannabinoid type-1 receptors (CB1Rs) that are found in many of the same brain regions as opioid receptors (Befort, 2015), including in the vlPAG where they are highly expressed (Wilson-Poe et al., 2012). Furthermore, infusions of synthetic cannabinoid receptor agonists into the ventricles, the PAG or the RVM all produce analgesia in naïve male rats (Lichtman et al., 1996; Meng et al., 1998). It is not known how THC vapor inhalation alters vlPAG function in experimentally naïve animals or in animal models of chronic inflammatory pain.

In humans, vaping cannabis and cannabinoid compounds is a common route of usage that is on the rise (Giroud et al., 2015; Lee et al., 2016; Trivers et al., 2019). Until recently, most rodent studies of THC effects on brain and behavior have not used vapor inhalation techniques, but THC and cannabis vapor techniques are becoming more common in preclinical neuroscience research. For example, THC and cannabidiol

(CBD) vapor inhalation models have been used to test cannabinoid effects on nociception, body temperature and drug discrimination in rats, and also for studies of cannabinoid drug pharmacokinetics (Hložek et al., 2017; Nguyen et al., 2018; Wiley et al., 2021; Moore et al., 2021a; 2021b). Here, we designed a series of studies to test the effect of chronic THC vapor inhalation on pain-related behaviors and vlPAG circuit function in adult male Wistar rats. We hypothesized that chronic THC vapor would have anti-hyperalgesic effects in rats with chronic inflammatory pain, and that it would produce disinhibition of vlPAG neurons.

Methods

Animals

Adult male (N=94) specific pathogen free Wistar rats (Charles River, Raleigh, NC) were housed in a humidity- and temperature-controlled (22 °C) vivarium on a 12 h light/12 h dark cycle (lights off at 8 a.m.). All rats were housed in groups of two. Rats were 8 weeks old upon arrival and acclimated for one week before start of experiments. Rats were handled daily prior to initiation of experimental protocols. Behavioral testing and vapor exposure occurred during the dark period. All procedures were approved by the Institutional Animal Care and Use Committee of the Louisiana State University Health Sciences Center and were in accordance with the National Institute of Health guidelines.

Drugs

Δ^9-tetrahydrocannabinol (THC) was supplied in ethanolic solution (200mg/mL) by the Research Triangle Institute (RTI) in conjunction with the U.S. National Institute on Drug Abuse (NIDA) Drug Supply Program. THC was administered at a dose of 100 mg THC diluted in propylene glycol (PG) vehicle (1 ml) via vapor inhalation during 1-hour daily sessions that occurred over 10 consecutive days.

Complete Freund's Adjuvant (CFA)

A localized chronic inflammatory pain state was established by injecting 150 µL of 50% complete Freund's adjuvant (Sigma) in 0.9% saline subcutaneously into the intraplantar surface of the left hind paw. This injection produced visible inflammation that resulted in thermal hyperalgesia and mechanical hypersensitivity (see *Results*). Control rats were injected with 150 µL of 0.9% saline into the left hind paw that produced no inflammation.

Nociception assays

For Experiment 1, pre-CFA and post-CFA thermal nociception and mechanical sensitivity were assessed over several sessions. The 3 sessions preceding CFA injections were averaged together to obtain pre-CFA baseline thermal nociception and mechanical sensitivity scores for each rat, and those data were used to counterbalance baseline pain-like behaviors in rats assigned to CFA and Saline groups. Following injection of CFA or Saline, rats were tested for 3 additional sessions of thermal nociception and mechanical sensitivity, and the scores obtained in those tests were used to assign rats to one of four groups that were counterbalanced for post-CFA pain-like behaviors. The four groups were: CFA and 100 mg THC vapor (N=8), Saline and

100 mg THC vapor (N=8), CFA and Vehicle (PG) vapor (N=12), and Saline and Vehicle (PG) vapor (N=12) groups.

During the 10 days of THC or PG vapor exposure (1 hour per day), rats were repeatedly tested for either thermal nociception or mechanical sensitivity in the Hargreaves and Von Frey tests respectively, across alternating days, as follows: Hargreaves tests were conducted on vapor days 2,5, and 8; Von Frey tests were conducted on vapor days 3, 6, and 9. All of those tests occurred 5 minutes after the end of vapor inhalation sessions. Hargreaves and Von Frey tests were repeated one final time on day 11 of the protocol at a time point that coincided with 24 hours after the 10^{th} and final vapor exposure session.

Hargreaves thermal sensitivity testing

Before all pre-CFA/saline and post-CFA/saline baseline nociception testing, animals were habituated to the behavior room for 30 minutes. Once room habituation was completed, rats were placed in 4 × 8 × 5 inch clear plexiglass enclosures on top of a glass pane suspended 8 inches above the table top. Thermal nociception threshold was measured by Hargreaves plantar test (Hargreaves Apparatus, Model 309, IITC Life Sciences), which measures the latency for each rat to withdraw its hind paw when stimulated by a halogen lamp heat source from underneath a glass pane. Paw withdrawal latency (PWL) in response to the application of thermal heat was recorded in seconds with a cutoff time of 20 seconds to prevent potential burn. Four readings were obtained from each rat in one session, two from each hind paw in an alternating manner

with at least 1 min between the readings. The readings were then averaged to determine a thermal nociception score for each hindpaw from each rat.

Von Frey mechanical sensitivity testing

Mechanical sensitivity was determined using automated Von Frey equipment (Ugo Basile, Italy) and obtaining pre-CFA and post-CFA baseline hind paw withdrawal thresholds. On experimental days where Von Frey and Hargreaves testing occurred on the same day (pre-CFA and post-CFA baseline days and day 11 post-vapor), Von Frey testing always occurred following Hargreaves testing. On these days, rats were acclimated to the test room for 30 minutes, tested for thermal nociception in the Hargreaves test, then acclimated for 15 minutes to individual plexiglass compartments set on top of a mesh stand and tested for mechanical sensitivity in the Von Frey test. In the Von Frey test, an automated device is used that applies a steel filament to the plantar surface of the hindpaw with gradually increasing force until the hindpaw is withdrawn (the withdrawal force is rounded to the nearest 0.1 g). For each rat on each test day, the filament was applied to each hindpaw twice (four total applications) in an alternating manner with at least 1 minute between each application and measurement. Measured values were averaged to determine a mechanical nociception score for each hindpaw from each rat on each test day.

THC Vapor Delivery

Seven days after the injection of CFA or saline, rats were placed in sealed exposure chambers (35 x 28 x 26 cm) manufactured by LJARI for 1-hour long vapor sessions. An

e-vape controller (Model SVS-200; 30.0 watts; La Jolla Alcohol Research, Inc., La Jolla, CA, USA) was scheduled to deliver 6 s puffs every 5 min from a Smok Baby Beast Brother TFV8 sub-ohm tank (fitted with the V8 X-Baby M2 0.25 Ω coil). The volume of PG vehicle or THC 100mg solution used was ~1 mL per 1-hour session. The chamber air was vacuum-controlled to flow ambient air through an intake valve at ~0.8 L per minute. The vapor cloud cleared from the chamber by 2 min after the puff delivery. Animals were exposed to THC or vehicle vapor for one hour daily for 10 days. Plasma was collected for analysis via tail bleeds immediately after the 1-hour session ended on days 1 and 10 in Experiment 1.

Plasma THC analysis

Tail blood samples (~500 µL) were collected by making a cut 1 mm at the tip of the tail; the same cut was used to collect blood from each rat immediately after the end of the 1-hour vapor session on days 1 and 10. Blood was collected in Eppendorf tubes and kept on ice until centrifugation. After centrifugation, plasma (~50 µL) was stored at -80°C until analysis.

Full method of THC analysis can be found in Baglot et al., 2021 (Baglot et al., 2021); in brief, plasma samples were thawed and 100 µL of sample was added directly to borosilicate glass tubes containing 2 ml of acetonitrile and 100 µL of internal standard (IS) stock solutions (IS contain THC-d3, 11-OH-THC-d3 and THC-COOH-d3 were dissolved in acetonitrile at 0.1 mg/mL; all d3 standards from Cerilliant, Round Rock, TX, USA). All samples were then sonicated in an ice bath for 30 min before being stored

overnight at -20°C to precipitate proteins. The next day samples were centrifuged at 1800 rpm at 4°C for 3-4 min to remove particulates and the supernatant from each sample was transferred to a new glass tube. Tubes were then placed under nitrogen gas to evaporate. Following evaporation, the tube sidewalls were washed with 250 µL acetonitrile in order to recollect any adhering lipids and then again placed under nitrogen gas to evaporate. Following complete evaporation, the samples were re-suspended in 100 µL of 1:1 methanol and deionized water. Resuspended samples went through two rounds of centrifugation (15000 rpm at 4°C for 20 min) to remove particulates and the supernatant transferred to a glass vial with a glass insert. Samples were then stored at -80°C until analysis by LC-MS / Multiple Reaction Monitoring (MRM). LC-MS/MS analysis was performed using an Eksigent Micro LC200 coupled to an AB Sciex QTRAP 5500 mass spectrometry (AB Sciex, Ontario, Canada) at the Southern Alberta Mass Spectrometry (SAMS) facility located at the University of Calgary, as previously described (Baglot et al., 2021). Analyte concentration (in pmol/µL) were normalized to sample volume and converted to ng/mL.

Electrophysiology

Under isoflurane anesthesia, rats were transcardially perfused with 100 mL room temperature (~25°C) NMDG artificial cerebrospinal fluid (aCSF) containing the following (in mM): 92 NMDG, 2.5 KCl, 1.25 NaH_2PO_4, 30 $NaHCO_3$, 20 HEPES, 25 glucose, 2 thiourea, 0.5 $CaCl_2$, 10 $MgSO_4 \cdot 7\ H_2O$, 5 Na-ascorbate, 3 Na-pyruvate. 300 µm-thick coronal sections containing the vlPAG were collected using a vibratome (Leica VT1200S, Nussloch, Germany). Sections were incubated in NMDG aCSF at 37°C for 12

min, then transferred to a room temperature holding aCSF solution containing the following (in mM): 92 NaCl, 2.5 KCl, 1.25 NaH_2PO_4, 30 $NaHCO_3$, 20 HEPES, 25 glucose, 2 thiourea, 2 $CaCl_2$, 2 $MgSO_4 \cdot 7\ H_2O$, 5 Na-ascorbate, 3 Na-pyruvate. Slices were allowed to recover for one hour prior to recording. Slices were visualized with oblique infrared light illumination**,** a w60 water immersion objective (LUMPLFLN60X/W, Olympus, Tokyo, Japan) and a CCD camera (Retiga 2000R, QImaging, Surrey, BC, Canada). Data were collected using the acquisition control software package Ephus (Suter et al., 2010).

At the time of recording slices were transferred to slice chamber in the electrophysiology rig in a recording aCSF kept at 30-32°C by an in-line heater. The recording solution consisted of (in mM): 119 NaCl, 2.5 KCl, 1.25 NaH_2PO_4, 24 $NaHCO_3$, 12.5 glucose, 2 $CaCl_2$, 2 $MgSO_4$. Whole-cell recordings were performed using borosilicate glass micropipettes (3–7MOhm) filled with internal solution containing (in mM): 130 K-gluconate, 10 HEPES, 10 Na_2-phosphocreatine, 4 $MgCl_2$, 4 Na_2-ATP, 0.4 Na-GTP, 3 ascorbic acid, 0.2 EGTA (pH 7.25, 290–295 mOsm). Electrical signals were amplified and digitized by a Multiclamp 700B amplifier (Molecular Devices, San Jose, CA). Recordings were sampled at 10 kHz and low pass Bessel filtered with a cutoff of 4 kHz. Signals were further filtered offline in Matlab with a cutoff of 2 kHz.

Synaptic Properties: To collect data regarding pre- and postsynaptic alterations resulting from TBI and inhibitor treatment, spontaneous excitatory postsynaptic currents (sEPSCs) were recorded. When whole-cell recording configuration was established, the

voltage was clamped at -50 mV and 5 min of spontaneous postsynaptic current was recorded. Blockers of glutamate receptors, CNQX (10 μM) + APV (50 μM) were circulating in the aCSF bath throughout all recordings. Spontaneous inhibitory postsynaptic events were detected in these recordings by thresholding rapid excursions in outward current; the average event amplitude and mean frequency over the 5 min recording period were quantified.

Intrinsic Properties: Because intrinsic subthreshold neural properties also contribute to integration of input synaptic signals and neural excitability, injury and/or treatment effects on intrinsic neural properties were assessed; specifically, input resistance, SAG fraction, and resting membrane potential (RMP) were measured. To estimate input resistance, holding current was recorded in voltage clamp mode with membrane voltage clamped at -70 mV. A -5 mV step was applied to the command voltage and the change in holding current, ΔI, was measured. The input resistance was estimated using Ohm's law, $R = \Delta V / \Delta I$. Rebound response to hyperpolarization activated inward current, known as the voltage SAG, was calculated as $\Delta V2 / \Delta V1$, where ΔV1 is the difference between pre-step baseline voltage (-70 mV) and the steady state voltage during step current injection, and ΔV2 is the difference between current step steady state voltage and the minimum voltage during current injection. Voltage SAG (Dembrow et al., 2010; Joshi et al., 2015) is reflective of subthreshold current mediated by HCN channels, also known as I_h. RMP was recorded in current clamp mode with injected current set at 0 pA.

Action Potential Generation Properties: Properties related to action potential generation were also examined, including spike threshold, firing rate, and firing rate-input gain. The spike threshold is the most depolarized membrane voltage level before the action potential excursion. In this study, it was defined as the voltage at which the second derivative (i.e. curvature) of the voltage was at its local maximal value. Input current steps of varying current amplitudes were delivered and the membrane voltage response to these current step inputs was recorded. Action potentials during each current step were counted and used to construct a firing rate-input (FI) curve. The FI curve gain was quantified by calculating the slope of the curve between 50 and 150 pA.

For experiments that tested the effect of MOR activation on inhibitory synaptic transmission, we recorded from vlPAG neurons in voltage clamp mode (@ -50 mV) and electrically stimulated nearby (~150 – 300 µm) vlPAG with a bipolar chromium wire electrode to evoke inhibitory postsynaptic currents (eIPSCs). vlPAG was stimulated and eIPSCs were recorded every 20 s for 10 mins to establish baseline amplitude. At this point DAMGO (100 nM) was delivered to the bath and eIPSCs were recorded for an additional 15 mins. Mean eIPSC amplitude during this period was estimated using eIPSC responses between 5 mins (or later if stable equilibrium was not reached at 5 min) and 15 mins of drug application.

Experiment 1: Effect of THC vapor exposure on thermal nociception and mechanical sensitivity

Experiment 1 was conducted in a group of male Wistar rats (N=40). Rats were baseline tested for thermal and mechanical sensitivity using HG and VF testing as described above. Rats were assigned to counterbalanced CFA (N=20) or saline (N=20) control groups dependent on the collected baseline data scores for thermal and mechanical nociception. Rats were then injected in the left hindpaw with CFA (N=20) or saline (N=20). HG and VF testing was repeated, and the resulting values were used to assign rats to either THC 100 mg or vehicle vapor control groups, with final groups of CFA and 100 mg THC vapor (N=8), saline and 100 mg THC vapor (N=8), CFA and vehicle vapor (N=12) or saline and vehicle vapor (N=12). 7 days after the injection of CFA or saline rats began 10 days of chronic vapor exposure. Rats were exposed to vapor for 1 hour daily, with tail bleeds occurring on days 1 and 10. Rats were tested for thermal sensitivity using HG (days 2,5, and 8) or mechanical sensitivity using VF (days 3,6, and 9) five minutes after the end of the hour-long vapor session. HG and VF testing was repeated for a final time 24 hours after the last vapor exposure session. Data were analyzed using 3-way RM ANOVAs where Pain and Vapor history were between-subjects factors and time was a within-subjects factor: one set of analyses included baseline and three vapor test days to assess acute THC vapor effects on behavior, and another set of analyses included three vapor days and the 24-hour post THC vapor time point to assess lasting THC vapor effects on behavior. Further analyses were done using 2-Way repeated measures on the same "acute" and "lasting" periods within CFA subjects and Saline subjects separately.

Experiment 2: Effect of THC vapor exposure on plasma THC concentrations over time

Experiment 2 was conducted using plasma obtained from the rats tested in Experiment 1. Tail blood collections occurred immediately after the end of THC vapor exposure sessions on days 1 and 10. Plasma samples were frozen and stored at -80°C until MS analysis. Three THC plasma concentration values were identified as outliers using the interquartile range (IQR) test: specifically, they were >1.5 x IQR above the 3rd quartile (Q3) value. All measurements (THC, 11-OH-THC and THC-COOOH) from these samples were excluded from analysis. Data were analyzed using 3-way RM ANOVA, where CFA and THC vapor were between-subjects factors and time (day 1 vs. day 10) was a within-subjects factor.

Experiment 3: Effects of CFA and THC vapor exposure on intrinsic properties and synaptic transmission in vlPAG neurons

Experiment 3 was conducted using a second group of male Wistar rats (N=44). Rats were injected in the left hindpaw with either CFA or saline. Seven days after the injection of CFA or Saline rats were exposed to either 100 mg THC or vehicle vapor during daily 1-hour sessions for 10 consecutive days. Twenty-four hours after the 10th and final vapor exposure session, rats were sacrificed for electrophysiological brain slice experiments. Electrophysiological data analysis and statistical analysis were performed in Matlab (MathWorks, Natick, MA). The group sizes are: Sal/Veh – 43 neurons (11 rats), Sal/THC – 44 neurons (8 rats), CFA/Veh – 41 neurons (11 rats), CFA/THC – 55 neurons (14 rats).

In the Sal/Veh group there were 11 rats, with an average of 3.9 neurons per rat. Statistical comparisons of electrophysiological parameters were performed using 2-way

ANOVAs where Pain condition and Vapor content were between-subjects factors. Post-hoc pairwise comparisons were performed using Tukey's honest significant difference (HSD). Statistics were performed on groups where individual samples correspond to individual neurons. The magnitude of main effects (for results with $p < 0.05$) were quantified using partial eta squared, η_p^2, which measures the proportion of variation in the dependent variable associated with its membership in an experimental group (Lakens, 2013).

Results

Experiment 1

CFA produced mechanical hypersensitivity and thermal hyperalgesia in rats

Injection of 150ul 50% CFA into the left hindpaw increased mechanical sensitivity and thermal nociception in rats. Rats treated with CFA had lower force thresholds recorded during the Von Frey test (**Fig. 2A**, $t(30) = 11.87$, $p<0.0001$) and lower paw withdrawal latency times recorded during the Hargreaves test (**Fig. 2B**, $t(30)=15.76$, $p<0.0001$) relative to saline treated rats. These data are illustrated in the BL timepoint of **Figures 2A and 2B**.

THC acute effects on mechanical sensitivity.

3-Way repeated-measures ANOVA, including BL and Vapor days, of mechanical sensitivity data for saline and CFA treated rats following vaporized THC or vehicle exposure (**Fig. 2A**) revealed no significant interactions or main effects for any variables: Time*Pain*Vapor $F(3,108) = 1.328$, $p=0.257$, Time*Vapor condition [$F(3,108) = 1.634$

p=0.186], Time*Pain condition [F(3,108) = 0.432, p = 0.731] or Time [F(3,108) = 0.393, p=0.758].

THC acute effects on mechanical sensitivity in CFA treated rats.

A 2-Way repeated measures ANOVA of mechanical sensitivity in CFA rats (**Fig. 2A**) showed a significant effect of THC treatment [F(1,18) = 5.679, p = 0.0284]. However, there was no significant effect of Time [F(3,54) = 0.2557, p = 0.8569] or a significant interaction of factors [F (3,54) = 0.2086, p = 0.8900].

THC acute effects on mechanical sensitivity in Saline treated rats.

A 2-Way repeated measures ANOVA of mechanical sensitivity in Saline rats showed that THC vapor exposure did not significantly alter mechanical sensitivity when compared to PG vehicle exposure (**Fig. 2A**). Analysis showed no significant effect of Time [F (3,54) = 0.4723, p = 0.6499], THC treatment [F (1,18) = 0.7703, p = 0.3917], or any interaction of factors [F (3,54) = 1.968, p = 0.1297]. Together these findings show that chronic THC Vapor does not alter mechanical nociception relative to baseline (i.e. no significant Time effect or significant interaction of factors with Time).

THC lasting effects on mechanical sensitivity.

3-Way repeated measures ANOVA, including Vapor days and 24hr post Vapor day, (**Fig. 2A**) showed no significant 3-way interactions for Time*Pain condition*Vapor condition [F(3,108)=3.288 p=0.078], no interactions for Time*Vapor condition [F(3,108)=0.675 p=0.417] or Time*Pain condition [F(1,36)=2.079 p=0.158], and no effect of Time [F(3,108)= 0.517 p=0.477].

THC lasting effects on mechanical sensitivity in CFA rats.

A 2-Way repeated measures ANOVA of mechanical sensitivity in CFA rats (**Fig. 2A**) revealed a significant effect of THC treatment [$F(1,18)= 7.425$ $p=0.0139$], but no significant effect of Time [$F(3,54)= 0.2793$ $p=0.6036$] and no interaction of factors [$F(3,54)=0.5261$ $p=0.4776$].

THC lasting effects on mechanical sensitivity in Saline rats.

Analysis of mechanical sensitivity in Saline rats 24 hours after the last THC or vehicle vapor exposure (**Fig. 2A**) showed no significant effects of THC treatment [$F(1,18)= 2.061$ $p=0.1682$] or Time [$F(3,54)= 2.191$ $p=0.1561$] and no interaction of effects [$F(3,54)= 3.258$ $p=0.0878$]. Together these findings show that chronic THC Vapor does not alter mechanical nociception 24 hours post Vapor compared to Vapor delivery days (i.e. no significant Time effect or significant interaction of factors with Time).

THC acute effects on thermal nociception

A 3-way repeated measures ANOVA, including BL and Vapor days, of thermal nociception data (**Fig. 2B**) for Saline and CFA treated rats revealed a significant interaction of Time*Vapor condition [$F(3,108)=6.061$ $p=0.001$], Time*Pain condition [$F(3,108)=8.840$ $p=0.000$], and a significant main effect of Time [$F(3,108)=8.450$ $p=0.000$]. However, no significant interaction was found between all three factors Time*Pain*Vapor [$F(3,108)=1.387$ $p=0.251$].

THC acute effects on thermal nociception in CFA treated rats.

THC vapor exposure rescued CFA induced thermal hyperalgesia (**Fig. 2B**). A 2-Way repeated measures ANOVA of thermal sensitivity in CFA rats showed a significant main effects of Time [$F(3,54)=19.69$ $p<0.0001$], THC treatment [$F(1,18)=28.75$ $p<0.0001$] and the interaction of factors [$F(3,54)=7.222$ $p=0.004$]. Post hoc tests confirmed that vapor THC (100 mg) exposure compared with PG vehicle increased paw withdrawal latency in CFA treated rats on vapor days 2, 5 and 8 ($p<.05$).

THC acute effects on thermal nociception in Saline treated rats.

THC (100 mg) vapor exposure in saline treated rats did not significantly alter thermal sensitivity when compared to PG vehicle vapor exposure (**Fig. 2B**). A 2-Way repeated measures ANOVA of thermal sensitivity in Saline rats showed no significant main effects of Time [$F(3,54)=0.4723$ $p=0.6499$], no significant main effect of THC treatment [F (THC $F(1,18)=3.959$ $p=0.0620$], and no interaction of factors [$F(3,54)=1.968$ $p=0.1297$]. Together these findings show that chronic THC Vapor affects thermal nociception relative to baseline, specifically in in CFA rats (i.e. significant Time effect and significant interaction of factors with Time).

THC lasting effects on thermal nociception.

3 -Way repeated measures ANOVA, including Vapor days and 24hr post Vapor day, of thermal nociception for saline and CFA rats (**Fig. 2B**) showed a significant interaction of Time*Pain condition [$F(3,108)=13.554$ $p=0.001$], a significant effect of Time [$F(3,108)=26.390$ $p=0.000$], but no interaction for Time*Vapor condition [$F(3,108)=1.944$

p=0.172] and no significant 3-way interaction for Time*Pain condition*Vapor condition [F(3,108)=1.947 p=0.171]

THC lasting effects on thermal nociception in CFA rats.

A 2-Way repeated measures ANOVA of thermal sensitivity in CFA rats (**Fig. 2B**) showed a significant effect of THC treatment [THC F(1,18)=6.783 p=0.0179] and a significant effect of Time [F(3,54)=28.78 p<0.001], but no significant interaction of factors [F(3,54)= 2.881 p=0.1069]

THC lasting effects on thermal nociception in Saline rats.

A 2-Way repeated measures ANOVA of thermal sensitivity in Saline rats (**Fig. 2B**) showed no significant effects of THC treatment [F(1,18)= 0.1197 p=0.7334] or Time [F(3,54)= 1.632 p=0.2176] and no interaction of factors [F(3,54)= 9.703e-007 p=0.992] Together these findings show that chronic THC Vapor affects thermal nociception 24 hours post Vapor compared to Vapor delivery days (i.e. significant THC effect and significant effect of Time).

Experiment 2

Plasma THC levels following THC vapor exposure days 1 and 10

A mixed effects analysis of plasma samples collected from CFA- and Saline-treated rats on days 1 and 10 following exposure to 100 mg THC vapor (**Fig. 3**) showed no significant effects of Pain condition [F(1,25)=0.1528 p=0.6991] or Time [F(1,25)=2.164 p=0.1538] and no interaction of factors [F(1,25)=0.8779 p=0.3577].

Experiment 3

We tested the effects chronic inflammation and chronic THC vapor on neural and synaptic properties in vlPAG neurons by performing whole cell recordings. Voltage and current recordings were performed to characterize measures of intrinsic excitability: resting membrane potential [RMP], input resistance (R_{input}) and voltage SAG. A 2-way ANOVA analysis of RMP data revealed no effect of Pain [$F(1,150) = 0.002$, $p = 0.9686$] or Vapor [$F(1,150) = 0.14$, $p = 0.7062$], and no interaction effect [$F(1,150) = 0.03$, $p = 0.8565$] (**Fig. 4A**). A 2-way ANOVA analysis of R_{input} data showed no main effect of Pain [$F(1,166) = 0.2$, $p = 0.6522$] or Vapor [$F(1,166) = 2.1$, $p = 0.1489$], and no interaction effect [$F(1,166) = 0.96$, $p = 0.3277$] (**Fig. 4B**). Figure 4C shows the characteristic rebound voltage excursion seen in some neurons following hyperpolarization caused by negative current steps, known as voltage SAG. A 2-way ANOVA analysis of SAG data showed no main effect of Pain [$F(1,173) = 0.3$, $p = 0.5996$] or Vapor [$F(1,173) = 2.3$, $p = 0.128$], and no interaction effect [$F(1,173) = 3.73$, $p = 0.0551$] (**Fig. 4D**). Figure 4E shows membrane voltage responses to current step inputs. Figure 4F shows the FI curve constructed from the number of action potentials during each current step. 2-way ANOVA analysis of the Firing rate @ 150 pA revealed a significant main effect of Vapor [$F(1,174) = 4.19$, $p = 0.0421$], with lower firing rates in the THC groups and an effect size of 0.024. There was no effect of Pain [$F(1,174) = 0.003$, $p = 0.9602$] or Pain x Vapor interaction effect [$F(1,174) = 0.54$, $p = 0.4638$] (**Fig. 4G**). Posthoc pairwise comparisons revealed no significant differences between individual groups. A 2-way ANOVA analysis of the gain of the firing rate curves, calculated between 50 and 150 pA

inputs, showed no main effect of Pain [$F(1,174) = 0.01$, $p = 0.9241$] or Vapor [$F(1,174) = 3.56$, $p = 0.061$], and no interaction effect [$F(1,174) = 0.59$, $p = 0.4435$] (**Fig. 4H**). Posthoc pairwise comparisons revealed no significant differences between individual groups.

Current clamp recordings were performed to characterize synaptic properties of vlPAG neurons: with blockers of glutamate receptors (APV [50 µM] and CNQX [10 µM]) we recorded postsynaptic currents while clamping the voltage at -50 mV (**Fig. 5A**) and detected unitary spontaneous inhibitory current events (**Fig. 5B**). The amplitude and frequency of these events was calculated to assess net inhibitory inputs to the recorded vlPAG neurons. 2-way ANOVA analysis of sIPSC amplitude data revealed a significant main effect of Vapor [$F(1,150) = 31.91$, $p = 0.0003$], with lower sIPSC amplitudes in the THC groups and an effect size of 0.085. There was no main effect of Pain [$F(1,150) = 0.1$, $p = 0.7473$], and no interaction effect [$F(1,150) = 0.5$, $p = 0.4811$] (**Fig. 5C**). Posthoc pairwise comparisons revealed significant differences between Sal/Veh and Sal/THC groups ($p < 0.01$) and Sal/THC and CFA/Veh groups ($p < 0.05$), with the means of the Sal/Veh and CFA/Veh groups being significantly larger than the Sal/THC group mean. A 2-way ANOVA analysis of sIPSC rate data revealed a main effect of Vapor [$F(1,150) = 8.23$, $p = 0.0047$], with lower sIPSC rates in the THC groups and an effect size of 0.052. There was no main effect of Pain [$F(1,150) = 0.23$, $p = 0.63334$] and no interaction effect [$F(1,150) = 8e^{-5}$ $p = 0.9927$] (**Fig. 5D**). Posthoc pairwise comparisons revealed no significant differences between individual groups.

We investigated action potential firing patterns to examine if there were firing phenotype-specific effects of THC Vapor on the parameters investigated, particularly firing rate response curves and synaptic properties. We found that recordings were easily divided based on the delay of first AP from current step onset. One population exhibited a short latency delay from current step onset (labeled 'Onset' neurons) while another displayed a distinctive longer latency delay from current step onset (labeled 'Delayed' neurons) (**Fig. 6A**). There were no significant differences in the proportion of these types between any of the experimental groups (**Fig. 6B**; Sal/Veh: n_{onset} = 27, $n_{delayed}$ = 16; Sal/THC: n_{onset} = 27, $n_{delayed}$ = 17; CFA/Veh: n_{onset} = 29, $n_{delayed}$ = 11; CFA/THC: n_{onset} = 38, $n_{delayed}$ = 15).

A 2-way ANOVA analysis of RMP data collected from Onset neurons revealed no main effect of Pain [$F(1,96) = 0.003$, $p = 0.958$] or Vapor [$F(1,96) = 0.63$, $p = 0.4286$], and no interaction effect [$F(1,96) = 1.2$, $p = 0.277$] (**Fig. 7A**). A 2-way ANOVA analysis of RMP data collected from Delayed neurons revealed no effect of Pain [$F(1,50) = 0.06$, $p = 0.8011$] or Vapor [$F(1,50) = 2.03$, $p = 0.1608$], and no Pain x Vapor interaction effect [$F(1,50) = 3.15$, $p = 0.0823$] (**Fig. 7B**). A 2-way ANOVA analysis of R_{input} data collected from Onset neurons revealed no main effect of Pain [$F(1,106) = 0.18$, $p = 0.676$] or Vapor [$F(1,106) = 0.22$, $p = 0.6433$], and no interaction effect [$F(1,106) = 0.37$, $p = 0.5426$] (**Fig. 7C**). A 2-way ANOVA analysis of R_{input} data collected from Delayed neurons revealed no main effect of Pain [$F(1,53) = 0.06$, $p = 0.8098$] or Vapor [$F(1,53) = 3.23$, $p = 0.0779$], and no interaction effect [$F(1,53) = 0.67$, $p = 0.416$] (**Fig. 7D**). A 2-way ANOVA analysis of SAG data collected from Onset neurons revealed no main

effect of Pain [F(1,112) = 0.26, p = 0.6122] or Vapor [F(1,112) = 2.47, p = 0.1186], and no interaction effect [F(1,112) = 1.29, p = 0.2578] (**Fig. 7E**). A 2-way ANOVA analysis of SAG data collected from Delayed neurons revealed no main effect of Pain [F(1,54) = 0.85, p = 0.3594] or Vapor [F(1,54) = 0.1, p = 0.751], and no interaction effect [F(1,54) = 3.08, p = 0.0851] (**Fig. 7F**).

Firing rate response curves from Onset neurons of different experimental groups appeared to overlap (**Fig. 8A**). A 2-way ANOVA analysis of firing rate @ 150 pA of Onset neurons revealed no main effect of Pain [F(1,115) = 0.08, p = 0.7756] or Vapor [F(1,115) = 0.31, p = 0.5814], and no interaction effect [F(1,115) = 0.78, p = 0.3781] (**Fig. 8B**). A 2-way ANOVA analysis of firing rate gain in Onset neurons revealed no main effect of Pain [F(1,115) = 0.1, p = 0.7546] or Vapor [F(1,115) = 0.01, p = 0.9086], and no interaction effect [F(1,115) = 0.89, p = 0.3484] (**Fig. 8C**). Firing rate response curves from Delayed neurons from THC Vapor rats appeared to be lower than the curves from PG Vehicle Vapor rats (**Fig. 8D**). A 2-way ANOVA analysis of firing rate @ 150 pA of Delayed neurons revealed a main effect of Vapor [F(1,55) = 9.78, p = 0.0028], with lower firing rates in the THC groups and an effect size of 0.151. There was no main effect of Pain [F(1,55) = 0.002, p = 0.969] and no interaction effect [F(1,55) = 0.11, p = 0.7408] (**Fig. 8E**). Posthoc pairwise comparisons revealed no significant differences between individual groups. A 2-way ANOVA analysis of firing rate gain of Delayed neurons revealed a main effect of Vapor [F(1,55) = 11.83, p = 0.0011], with lower firing rate gain in the THC groups and an effect size of 0.177. There was no main effect of Pain [F(1,55) = $9e^{-4}$, p = 0.9763] and no interaction effect [F(1,55) = 0.18, p =

0.672] (**Fig. 8F**). Posthoc pairwise comparisons revealed no significant differences between individual groups.

We applied the same phenotype classification to the synaptic data to determine if different type of neurons exhibited different effects of Pain and Vapor on synaptic properties in vlPAG neurons. A 2-way ANOVA analysis of sIPSC amplitude data collected from Onset neurons revealed no main effect of Pain [$F(1,101) = 1.13$, $p = 0.291$] or Vapor [$F(1,101) = 2.3$, $p = 0.1325$], and no interaction effect [$F(1,101) = 0.002$, $p = 0.9664$] (**Fig. 9A**). A 2-way ANOVA analysis of sIPSC amplitude data collected from Delayed neurons revealed a main effect of Vapor [$F(1,45) = 16.99$, $p = 0.0002$] with lower sIPSC amplitudes in the THC groups and an effect size of 0.274. There was no effect of Pain [$F(1,45) = 1.28$, $p = 0.2636$] and no interaction effect [$F(1,45) = 0.17$, $p = 0.6827$] (**Fig. 9B**). Posthoc pairwise comparisons revealed significant differences between Sal/Veh and Sal/THC groups ($p < 0.01$) and Sal/Veh and CFA/THC groups ($p < 0.01$). A 2-way ANOVA analysis of sIPSC rate data collected from Onset neurons revealed no main effect of Pain [$F(1,101) = 0.1$, $p = 0.7531$] or Vapor [$F(1,101) = 0.51$, $p = 0.4761$] and no interaction effect [$F(1,101) = 0.07$, $p = 0.7866$] (**Fig. 9C**). A 2-way ANOVA analysis of sIPSC rate data collected from Delayed neurons revealed a main effect of Vapor [$F(1,45) = 18.8$, $p = 0.0001$] with lower sIPSC rates in the THC groups and an effect size of 0.295. There was no effect of Pain [$F(1,45) = 0.02$, $p = 0.8969$] and no interaction effect [$F(1,45) = 0.08$, $p = 0.7791$] (**Fig. 9D**). Posthoc pairwise comparisons revealed significant differences between Sal/Veh and Sal/THC groups ($p <$

0.05), Sal/Veh and CFA/THC groups ($p < 0.05$), Sal/THC and CFA/Veh groups ($p < 0.05$) and CFA/Veh and CFA/THC groups ($p < 0.05$).

To test the effect of MOR agonism on synaptic transmission in the vlPAG of rats treated with CFA and/or THC Vapor, we recorded vlPAG neurons in voltage clamp mode at -50 mV and electrically stimulated nearby vlPAG tissue to evoke IPSCs (eIPSCs). eIPSC responses were recorded and amplitudes were calculated in the aCSF bath, followed by bath application of DAMGO (100 nM) (**Fig. 10A**). eIPSC responses were typically attenuated after bath application of DAMGO (**Fig. 10B**). We quantified the suppressive effect of DAMGO on electrically evoked inhibition by dividing the mean eIPSC amplitude in the DAMGO conditions by the mean amplitude during the baseline condition. A 2-way ANOVA analysis of relative post/pre DAMGO amplitude revealed a main effect of Vapor [$F(1,35) = 8.35$, $p = 0.0066$], with lower pre/post ratios in the THC groups and an effect size of 0.193. There was no effect of Pain [$F(1,53) = 0.09$, $p = 0.7655$] and no interaction effect [$F(1,35) = 0.24$, $p = 0.6298$] (**Fig. 10C**), suggesting that Vapor history modulates MOR responses to agonism in the vlPAG, regardless of pain treatment. There were no posthoc differences observed between individual group datasets.

Discussion

Although cannabinoids have been identified as a possible alternative to opioids for the treatment of chronic pain, little is known about the site(s) and mechanism(s) of action for THC vapor inhalation effects on pain-related outcomes, nor about THC vapor dosing regimens and/or duration of THC vapor effects on pain-related outcomes. This study

was designed to examine the anti-nociceptive effects of THC exposure using an animal model of chronic inflammatory pain (CFA). The current study shows that chronic exposure to vaporized THC (100 mg/mL) one hour daily for 10 consecutive days acutely and repeatedly rescues CFA-induced thermal hyperalgesia in male Wistar rats, and that this effect lasts at least 24 hours after termination of THC vapor exposure. THC vapor exposure did not alter thermal nociception in saline-treated male Wistar control rats. Contrary to our hypothesis, chronic THC vapor inhalation did not rescue mechanical hypersensitivity in CFA-treated rats.

We also report that chronic THC vapor exposure alters intrinsic and synaptic properties of vlPAG neurons, whereas CFA treatment did not affect these outcome measures. Specifically, THC vapor history reduced firing rate, firing rate gain, sIPSC amplitude and sIPSC frequency in vlPAG neurons of rats sacrificed 24 hours after termination of the 10^{th} day of vapor exposure. Furthermore, these effects were found specifically in vlPAG neurons that exhibited a delayed-firing phenotype, but not in neurons that exhibited an onset-firing phenotype. Our quantification of effect sizes in the electrophysiological measures exhibiting main effects showed that the reduction of inhibitory synaptic amplitude and rates were approximately twice as large as reductions in the firing rates of the same neurons. This suggests that chronic THC vapor inhalation may activate descending pain modulation pathways via disinhibition of late-firing vlPAG neurons. Finally, we report that the mu-opioid receptor agonist DAMGO reduces presynaptic inhibition in the vlPAG of all experimental groups, as expected. Intriguingly, we observed a larger suppression of synaptic inhibition in vlPAG neurons recorded from

rats that had a history of chronic THC vapor exposure, independent of inflammatory pain condition. Prior work showed that repeated pre-treatment with cannabinoids (systemic injection or site-specific injection into vlPAG) for 2 consecutive days prior, enhances thermal anti-nociception by morphine in pain-naive male rats (Wilson et al., 2008; Wilson-Poe et al., 2013). Prior work also showed that CFA alters tonic GABAergic currents and miniature spontaneous postsynaptic current events in vlPAG neurons of female rats, but not male rats (Tonsfeldt et al., 2016). More recently, it was reported that CFA increases action potential firing rates in phasic-firing vlPAG neurons recorded from male and female rats (McPherson et al., 2021). Our ongoing studies are repeating the current set of experiments in adult female Wistar rats, and also following up on the firing-phenotype-specific neural effects observed in the vlPAG in the current study.

The CB1 receptor is highly expressed throughout the periaqueductal gray (Wilson-Poe et al., 2012). CFA treatment leads to a decrease in CB1R-mediated suppression of synaptic inhibition in vlPAG of rats (Bouchet and Ingram, 2020), and repeated cannabinoid exposures may downregulate CB1R in the rat brain (Breivogel et al., 1999). Our observation of chronic THC vapor-induced suppression of spontaneous synaptic inhibition in vlPAG (independent of pain condition) may suggest one potential mechanism whereby cannabinoids exert opioid-sparing effects, that is, by increasing the sensitivity of vlPAG neurons to opioid drug effects on inhibitory transmission.

All acute thermal nociception and mechanical sensitivity testing occurred 5 minutes after the end of vapor exposure sessions. Previous studies reported anti-nociceptive effects

of vaporized THC in “pain-naïve” rats using the tail flick assay at this time point (Javadi-Paydar et al., 2018; Nguyen et al., 2018). Using the same test, another recent study from the same group reported that maximal anti-nociceptive effects occurred 60 minutes after the end of THC vapor exposure in male Wistar rats (Moore et al., 2021a). Aside from the fact that we used different nociception assays in the present set of studies, it is possible that THC vapor effects may have differed if we delayed testing for thermal nociception and mechanical sensitivity. It is important to re-emphasize that we observed THC vapor attenuation of thermal hyperalgesia in CFA rats, but no specific effect of THC vapor on mechanical hypersensitivity in CFA rats. Evidence shows that different peripheral signaling pathways differentially affect distinct classes of nociceptors (Peirs and Seal, 2016): for example, selective ablation of receptors expressing Mas-related G protein-couple receptor subtype D (MRGPRD) attenuates mechanical nociception (Cavanaugh et al., 2009), while ablation of receptors expressing calcitonin gene-related peptide (CGRP), which partially overlaps with thermosensors TRPV1 and TRPM3 receptor expression, attenuates thermal nociception (McCoy et al., 2013). Less is known about differential circuit involvement in these distinct types of pain processes centrally, but it has been proposed that distinct circuit elements in the vlPAG regulate thermal nociception and mechanical sensitivity (Samineni et al., 2017). In that study, mechanical sensitivity in rats was insensitive to global chemogenetic activation of vlPAG neurons, inhibition of GABAergic vlPAG neurons and activation of glutamatergic vlPAG neurons, while thermal nociception was sensitive to bidirectional chemogenetic manipulation in all of those scenarios (Samineni et al., 2017). Future studies will test 1) whether these THC vapor effects are truly specific to thermal outcome measures, 2) the

site of action (central vs. peripheral; ascending vs. descending CNS pathways) that is critical for mediating THC vapor effects on pain-related outcomes in rats, and 3) whether the effects observed here in males are also observable in adult female rats.

Different groups have argued for the relative importance of GABAergic vs glutamatergic synaptic transmission being the primary mechanism for vlPAG-to-RVM circuit-mediated antinociception. For example, in the vlPAG of rats, global activation of vlPAG induces antinociception (Samineni et al., 2017), glutamatergic neuron activation also induces antinociception, whereas GABAergic neuron activation promotes nociception (Samineni et al., 2017). In seeming contrast to this finding, anatomical studies reveal that a majority (~71%) of vlPAG fibers that contact RVM neurons are GABAergic, and that this proportion is observed in ON cells, OFF cells and neutral cells in the RVM of mice (Morgan et al., 2008). Conversely, another study in mice showed that GABAergic neurons in the vlPAG were non-overlapping with retrogradely labeled RVM-projecting neurons, and that opioid-mediated analgesia depended on suppression of spiking activity of GABAergic neurons in the vlPAG, but that this effect was independent of presynaptic suppression of inhibition onto RVM-projecting neurons (Park et al., 2010). To our knowledge, there are currently no data from paired recordings that demonstrate a microcircuit involving a local inhibitory interneuron and an excitatory RVM-projecting neuron in vlPAG. It is well established that opioid receptor activation suppresses presynaptic inhibition in the vlPAG (Vaughan et al., 1997; Ingram et al., 1998), an effect that we replicated here. RVM-projecting vlPAG neurons are not directly inhibited by opioids via GIRKs (Osborne et al., 1996), while a fraction of unidentified (i.e., projection-

nonspecific) neurons in the vlPAG exhibit GIRK-mediated suppression of activity (Vaughan et al., 2003). These seemingly contradictory results may be reconciled by moving beyond amino acid neurotransmitters and examining pain effects on specific subsets of vlPAG neurons classified according to electrophysiological properties or other aspects of their molecular signature, as well as the effects of those neuronal subsets on pain-related outcomes *in vivo*.

Our study represents the first characterization of late-firing neurons in the vlPAG of rodents. In the BLA, late-firing neurons comprise ~22% of parvalbumin-positive (PV^+) local inhibitory interneurons (Woodruff and Sah, 2007). Late-firing phenotype neurons have been observed in the central amygdala, primarily in the lateral subdivision (Martina et al., 1999; Lopez de Armentia and Sah, 2004; Amano et al., 2012). A subset of both protein kinase C delta-positive ($PKC\delta^+$) and somatostatin-positive (SOM^+) neurons in the CeA of mice exhibit late-firing phenotypes (Ciocchi et al., 2010; Haubensak et al., 2010; Amano et al., 2012). In the CeA of mice, SOM^+ late-firing neurons have higher excitability than $PKC\delta^+$ late-firing neurons, but this difference is abolished in a sciatic nerve cuff model of neuropathic pain 6-14 days after injury (Adke et al., 2021). In the same model of neuropathic pain, $PKC\delta^+$ CeA neurons were pro-nociceptive and this seemed to be due to an increase in excitability of late-firing $PKC\delta^+$ but not regular-spiking $PKC\delta^+$ neurons (Wilson et al., 2019). Finally, in a mouse model of chronic inflammatory pain, late-firing vlPAG-projecting neurons in the CeA exhibited no changes 1 day after CFA injection into the hindpaw (Li and Sheets, 2018). It is not clear how cell firing phenotypes of different vlPAG neuron subsets is related to 1) projection targets of

those neurons, 2) alterations by chronic inflammatory (or neuropathic) pain, 3) opioid drug sensitivity, 4) THC sensitivity, 5) pain-related behaviors, or combinations of these factors. For example, if the role of these cells is similar to that of late-firing PKCδ^{+} neurons in the CeA (i.e., pro-nociceptive), then reduction of their firing activity via reductions in firing rate response and firing rate gain may have anti-nociceptive effects.

Here, we showed that CFA produces thermal hyperalgesia and mechanical hypersensitivity in adult male Wistar rats. Chronic THC vapor inhalation reversed thermal hyperalgesia, but not mechanical hypersensitivity, in rats treated with CFA. Chronic THC vapor inhalation also modulated intrinsic and synaptic properties of vlPAG neurons, and some of these effects were specific to neurons with a delayed-firing phenotype. Finally, we report that chronic THC vapor inhalation enhanced the suppressive effect of a mu-opioid receptor agonist on synaptic inhibition in the vlPAG. Future work will determine the potential role of specific vlPAG cell subtypes in mediating chronic inflammation and THC vapor inhalation effects on pain-related outcomes.

Figure Captions

Figure 1: Timelines for Experiment 1 (top) and Experiment 2 (bottom).

Figure 2: Effects of Pain condition and chronic Vapor on mechanical and thermal nociception. (**A**) Behavioral data for Mechanical Sensitivity Baseline, Vapor Days 3,6, 9 and 24 hours after the last vapor exposure. 3-Way repeated measures ANOVAs reveal no effect of THC Vapor history on mechanical sensitivity. (**B**) Thermal Nociception Baseline, Vapor Days 2,5, 8 and 24 hours after the last vapor exposure. 3-Way repeated measures ANOVAs reveal acute and lasting effects of THC vapor on thermal nociception.

Figure 3: Plasma THC and THC metabolites Analysis following vapor exposure days 1 and 10. (**A**) A mixed effects analysis of plasma samples collected from CFA and Saline treated rats on days 1 and 10 following exposure to 100 mg THC vapor (Fig. 3) showed no significant effects of Pain condition [$F(1,25)=0.1528$ $p=0.6991$] or Time [$F(1,25)=2.164$ $p=0.1538$] and no interaction of factors [$F(1,25)=0.8779$ $p=0.3577$] in THC plasma levels. Analysis of THC metabolites showed no significant effects of Pain condition [$F(1,13)=0.008842$ $p=0.9265$] or Time [$F(1,12)= 0.3816$ $p=0.5483$] and no interaction of factors [$F(1,12)=1.085$] on 11-OH-THC levels and no significant effects of Pain condition [$F(1,13)=0.02756$ $p=0.8707$] or Time [$F(1,12)=1.451$ $p=0.2516$] or interaction of factors [$F(1,12)=0.1838$ $p=0.6757$] on THC-COOH levels.

Figure 4: Effects of Pain and Vapor on intrinsic properties of vlPAG neurons. 2-Way ANOVAs show: (**A**) no effect of Pain [$F(1,150) = 0.002$, $p = 0.9686$] or Vapor [$F(1,150) = 0.14$, $p = 0.7062$] on RMP, (**B**) no effect of Pain [$F(1,166) = 0.2$, $p = 0.6522$] or Vapor [$F(1,166) = 2.1$, $p = 0.1489$] on R_{input}, and (**C,D**) no effect of Pain [$F(1,173) = 0.3$, $p = 0.5996$] or Vapor [$F(1,173) = 2.3$, $p = 0.128$] on SAG. (**E**) An example set of voltage responses to injected current steps of different magnitudes. (**F**) Mean firing Rate response curves of vlPAG neurons to injected current. (**G**) There was a main effect of Vapor on firing rate in vlPAG neurons [$F(1,174) = 4.19$, $p = 0.0421$]. (**H**) There was no main effect of Pain [$F(1,174) = 0.01$, $p = 0.9241$] or THC vapor [$F(1,174) = 3.56$, $p = 0.061$] on firing rate gain in vlPAG neurons.

Figure 5: Effects of Pain and Vapor of synaptic properties in vlPAG neurons. (**A**) An example current traces from a vlPAG neuron with membrane voltage clamped at -50 mV. (**B**) An example average inhibitory postsynaptic current event trace. (**C**) 2-Way ANOVA revealed a main effect of Vapor on sIPSC amplitude [$F(1,150) = 31.91$, $p = 0.0003$]. (**D**) There was also a main effect of Vapor on sIPSC rate [$F(1,150) = 8.23$, $p = 0.0047$]. $^*p < 0.05$, $^{**}p < 0.01$.

Figure 6: Action potential firing phenotype classification of vlPAG neurons. (**A**) Neurons in vlPAG displayed one of two different firing types based on the latency to first spike after the onset of injected depolarizing current. “Onset” neurons responded with action potentials at short latencies, while “Delayed” neurons responded with

conspicuously longer latencies. (**B**) The proportion of Onset neurons (~2/3) and Delayed neurons (~1/3) was not significantly different for any experimental group.

Figure 7: Firing phenotype-specific effects of Pain and Vapor on intrinsic properties of vlPAG neuron. (**A**) 2-Way ANOVA shows no main effect of Pain [$F(1,96) = 0.003$, $p = 0.958$] or Vapor [$F(1,96) = 0.63$, $p = 0.4286$] on RMP in Onset vlPAG neurons. (**B**) There is no main effect of Pain [$F(1,50) = 0.06$, $p = 0.8011$] or Vapor [$F(1,50) = 2.03$, $p = 0.1608$] on RMP in Delayed neurons. (**C**) There is no main effect of Pain [$F(1,106) = 0.18$, $p = 0.676$] or Vapor [$F(1,106) = 0.22$, $p = 0.6433$] on R_{input} in Onset neurons. (**D**) There is no main effect of Pain [$F(1,53) = 0.06$, $p = 0.8098$] or Vapor [$F(1,53) = 3.23$, $p = 0.0779$] on R_{input} in Delayed neurons. (**E**) There is no main effect of Pain [$F(1,112) = 0.26$, $p = 0.6122$] or Vapor [$F(1,112) = 2.47$, $p = 0.1186$] on SAG in Onset neurons. (**F**) There is no main effect of Pain [$F(1,54) = 0.85$, $p = 0.3594$] or Vapor [$F(1,54) = 0.1$, $p = 0.751$] on SAG in Delayed neurons.

Figure 8: Firing phenotype-specific effects of Pain and Vapor on action potential response properties. (**A**) Mean firing rate response curves of Onset vlPAG neurons to injected current. 2-Way ANOVAs show: (**B**) no effect of Pain [$F(1,115) = 0.08$, $p = 0.7756$] or Vapor [$F(1,115) = 0.31$, $p = 0.5814$] on firing rate, and (**C**) no effect of Pain [$F(1,115) = 0.1$, $p = 0.7546$] or Vapor [$F(1,115) = 0.01$, $p = 0.9086$] on firing rate gain in vlPAG Onset neurons. (**D**) Mean firing rate response curves of vlPAG neurons to injected current. (**E)** There was a main effect of Vapor on firing rate in vlPAG Delayed neurons [$F(1,55) = 9.78$, $p = 0.0028$]. (**F**) There was a main effect of Vapor on firing rate gain in vlPAG Delayed neurons [$F(1,55) = 11.83$, $p = 0.0011$].

Figure 9: Firing phenotype-specific effects of Pain and Vapor on synaptic properties of vlPAG neurons. (**A**) 2-Way ANOVA shows no main effect of Pain [$F(1,101) = 1.13$, $p = 0.291$] or Vapor [$F(1,101) = 0.002$, $p = 0.9664$] on sIPSC amplitude in Onset vlPAG neurons. (**B**) There was a main effect of Vapor on sIPSC amplitude in vlPAG Delayed neurons [$F(1,45) = 16.99$, $p = 0.0002$]. (**C**) There was no main effect of Pain [$F(1,101) = 0.1$, $p = 0.7531$] or Vapor [$F(1,101) = 0.51$, $p = 0.4761$] on sIPSC rate in vlPAG Onset neurons. (**D**) There was a main effect of Vapor on sIPSC rate in vlPAG Delayed neurons [$F(1,45) = 18.8$, $p = 0.0001$]. *$p < 0.05$, **$p < 0.01$.

Figure 10: Effects of Pain and Vapor on suppression on presynaptic inhibition by DAMGO. (**A**) Example eIPSC traces showing suppression of presynaptic inhibition after DAMGO (100 nM). (**B**) eIPSCs were recorded periodically every 20 sec for 40 mins. Baseline eIPSCs were recording for 10 mins after which DAMGO (100 nM) was applied to the bath. (**C**) 2-way ANOVA shows a main effect of Vapor [$F(1,35) = 8.35$, $p = 0.0066$] on DAMGO suppression of eIPSC amplitude.

References

Adke AP, Khan A, Ahn H-S, Becker JJ, Wilson TD, Valdivia S, Sugimura YK, Martinez Gonzalez S, Carrasquillo Y (2021) Cell-Type Specificity of Neuronal Excitability and Morphology in the Central Amygdala. eNeuro 8:ENEURO.0402–20.2020.

Amano T, Amir A, Goswami S, Paré D (2012) Morphology, PKCδ expression, and synaptic responsiveness of different types of rat central lateral amygdala neurons. J Neurophysiol 108:3196–3205.

Baglot SL, Hume C, Petrie GN, Aukema RJ, Lightfoot SHM, Grace LM, Rho JM, Borgland SL, McLaughlin RJ, Brechenmacher L, Hill MN (2021) Pharmacokinetics and Central Accumulation of Delta-9-Tetrahydrocannabinol (THC) and its Bioactive Metabolites Are Influenced by Route of Administration and Sex. bioRxiv doi:10.1101/2021.07.02.450963.

Baron EP, Lucas P, Eades J, Hogue O (2018) Patterns of medicinal cannabis use, strain analysis, and substitution effect among patients with migraine, headache, arthritis, and chronic pain in a medicinal cannabis cohort. J Headache Pain 19:37–28.

Basbaum AI, Fields HL (1984) Endogenous pain control systems: brainstem spinal pathways and endorphin circuitry. Annu Rev Neurosci 7:309–338.

Befort K (2015) Interactions of the opioid and cannabinoid systems in reward: Insights from knockout studies. Front Pharmacol 6:6.

Boehnke KF, Litinas E, Clauw DJ (2016) Medical Cannabis Use Is Associated With Decreased Opiate Medication Use in a Retrospective Cross-Sectional Survey of Patients With Chronic Pain. J Pain 17:739–744.

Bouchet CA, Ingram SL (2020) Cannabinoids in the descending pain modulatory circuit: Role in inflammation. Pharmacol Ther 209:107495.

Bradford AC, Bradford WD (2017) Medical Marijuana Laws May Be Associated With A Decline In The Number Of Prescriptions For Medicaid Enrollees. Health Aff (Millwood) 36:945–951.

Breivogel CS, Childers SR, Deadwyler SA, Hampson RE, Vogt LJ, Sim-Selley LJ (1999) Chronic delta9-tetrahydrocannabinol treatment produces a time-dependent loss of cannabinoid receptors and cannabinoid receptor-activated G proteins in rat brain. J Neurochem 73:2447–2459.

Cavanaugh DJ, Lee H, Lo L, Shields SD, Zylka MJ, Basbaum AI, Anderson DJ (2009) Distinct subsets of unmyelinated primary sensory fibers mediate behavioral responses to noxious thermal and mechanical stimuli. PNAS 106:9075–9080.

Ciocchi S, Herry C, Grenier F, Wolff SBE, Letzkus JJ, Vlachos I, Ehrlich I, Sprengel R, Deisseroth K, Stadler MB, Müller C, Lüthi A (2010) Encoding of conditioned fear in central amygdala inhibitory circuits. Nature 468:277–282.

Cooper ZD, Bedi G, Ramesh D, Balter R, Haney M (2018) Impact of co-administration of oxycodone and smoked cannabis on analgesia and abuse liability. Neuropsychopharmacology 43:2046–2055.

Dembrow NC, Chitwood RA, Johnston D (2010) Projection-Specific Neuromodulation of Medial Prefrontal Cortex Neurons. J Neurosci 30:16922–16937.

Giroud C, de Cesare M, Berthet A, Varlet V, Concha-Lozano N, Favrat B (2015) E-Cigarettes: A Review of New Trends in Cannabis Use. Int J Environ Res Public Health 12:9988–10008.

Guindon J, Hohmann AG (2009) The endocannabinoid system and pain. CNS Neurol Disord Drug Targets 8:403–421.

Haubensak W, Kunwar PS, Cai H, Ciocchi S, Wall NR, Ponnusamy R, Biag J, Dong H-W, Deisseroth K, Callaway EM, Fanselow MS, Lüthi A, Anderson DJ (2010) Genetic dissection of an amygdala microcircuit that gates conditioned fear. Nature 468:270–276.

Hirakawa N, Tershner SA, Fields HL (1999) Highly delta selective antagonists in the RVM attenuate the antinociceptive effect of PAG DAMGO. NeuroReport 10:3125–3129.

Hložek T, Uttl L, Kadeřábek L, Balíková M, Lhotková E, Horsley RR, Nováková P, Šíchová K, Štefková K, Tylš F, Kuchař M, Páleníček T (2017) Pharmacokinetic and behavioural profile of THC, CBD, and THC+CBD combinatio n after pulmonary, oral, and subcutaneous administration in rats and confirmation of conversion in vivo of CBD to THC. Eur Neuropsychopharmacol:1–16.

Ingram SL, Vaughan CW, Bagley EE, Connor M, Christie MJ (1998) Enhanced opioid efficacy in opioid dependence is caused by an altered signal transduction pathway. J Neurosci 18:10269–10276.

Javadi-Paydar M, Nguyen JD, Kerr TM, Grant Y, Vandewater SA, Cole M, Taffe MA (2018) Effects of Δ9-THC and cannabidiol vapor inhalation in male and female rats. Psychopharmacology (Berl) 235:2541–2557.

Joshi A, Joshi A, Middleton JW, Middleton JW, Anderson CT, Anderson CT, Borges K, Borges K, Suter BA, Suter BA, Shepherd GMG, Shepherd GMG, Tzounopoulos T, Tzounopoulos T (2015) Cell-Specific Activity-Dependent Fractionation of Layer 2/3->5B Excitatory Signaling in Mouse Auditory Cortex. J Neurosci 35:3112–3123 Available at: http://eutils.ncbi.nlm.nih.gov/entrez/eutils/elink.fcgi?dbfrom=pubmed&id=25698747&retmode=ref&cmd=prlinks.

Lakens D (2013) Calculating and reporting effect sizes to facilitate cumulative science: a practical primer for t-tests and ANOVAs. Front Psychol 4:1–12.

Lee DC, Crosier BS, Borodovsky JT, Sargent JD, Budney AJ (2016) Online survey characterizing vaporizer use among cannabis users. Drug Alcohol Depend 159:227–233.

Li C, Sugam JA, Lowery-Gionta EG, McElligott ZA, McCall NM, Lopez AJ, McKlveen JM, Pleil KE, Kash TL (2016) Mu Opioid Receptor Modulation of Dopamine Neurons in the Periaqueductal Gray/Dorsal Raphe: A Role in Regulation of Pain. Neuropsychopharmacology 41:2122–2132.

Li JN, Sheets PL (2018) The central amygdala to periaqueductal gray pathway comprises intrinsically distinct neurons differentially affected in a model of inflammatory pain. J Physiol 596:6289–6305.

Lichtman AH, Cook SA, Martin BR (1996) Investigation of brain sites mediating cannabinoid-induced antinociception in rats: evidence supporting periaqueductal gray involvement. J Pharmacol Exp Ther 276:585–593.

Lopez de Armentia M, Sah P (2004) Firing properties and connectivity of neurons in the rat lateral central nucleus of the amygdala. J Neurophysiol 92:1285–1294.

Loyd DR, Morgan MM, Murphy AZ (2007) Morphine preferentially activates the periaqueductal gray-rostral ventromedial medullary pathway in the male rat: a potential mechanism for sex differences in antinociception. Neuroscience 147:456–468.

Mammen G, Rehm J, Rueda S (2016) Vaporizing cannabis through e-cigarettes: Prevalence and socio-demographic correlates among Ontario high school students. Can J Public Health 107:e337–e338.

Martina M, Royer S, Pare D (1999) Physiological properties of central medial and central lateral amygdala neurons. J Neurophysiol 82:1843–1854.

McCoy ES, Taylor-Blake B, Street SE, Pribisko AL, Zheng J, Zylka MJ (2013) Peptidergic CGRPα primary sensory neurons encode heat and itch and tonically suppress sensitivity to cold. Neuron 78:138–151.

McPherson KB, Bouchet CA, Ingram SL (2021) Physiologically distinct neurons within the ventrolateral periaqueductal gray are not defined by mu-opioid receptor expression but are differentially activated by persistent inflammation.

Meng ID, Manning BH, Martin WJ, Fields HL (1998) An analgesia circuit activated by cannabinoids. Nature 395:381–383.

Millan MJ (2002) Descending control of pain. Prog Neurobiol 66:355–474.

Moore CF, Davis CM, Harvey EL, Taffe MA, Weerts EM (2021a) Appetitive, antinociceptive, and hypothermic effects of vaped and injected Δ-9-tetrahydrocannabinol (THC) in rats: exposure and dose-effect comparisons by strain and sex. Pharmacol Biochem Behav 202:173116.

Moore CF, Weerts EW, 2021 (2021b) Cannabinoid tetrad effects of oral Δ9-tetrahydrocannabinol (THC) and cannabidiol (CBD) in male and female rats: sex, dose-effects and time course evaluations. bioRxiv doi:10.1101/2021.05.11.443601.

Morean ME, Kong G, Camenga DR, Cavallo DA, Krishnan-Sarin S (2015) High School Students' Use of Electronic Cigarettes to Vaporize Cannabis. Pediatrics 136:611–616.

Morean ME, Lipshie N, Josephson M, Foster D (2017) Predictors of Adult E-Cigarette Users Vaporizing Cannabis Using E-Cigarettes and Vape-Pens. Subst Use Misuse 52:974–981.

Morgan MM, Whittier KL, Hegarty DM, Aicher SA (2008) Periaqueductal gray neurons project to spinally projecting GABAergic neurons in the rostral ventromedial medulla. Pain 140:376–386.

Nguyen JD, Grant Y, Kerr TM, Gutierrez A, Cole M, Taffe MA (2018) Tolerance to hypothermic and antinoceptive effects of ∆9-tetrahydrocannabinol (THC) vapor inhalation in rats. Pharmacol Biochem Behav 172:33–38.

Nielsen S, Sabioni P, Trigo JM, Ware MA, Betz-Stablein BD, Murnion B, Lintzeris N, Khor KE, Farrell M, Smith A, Le Foll B (2017) Opioid-Sparing Effect of Cannabinoids: A Systematic Review and Meta-Analysis. Neuropsychopharmacology 42:1752–1765.

Osborne PB, Vaughan CW, Wilson HI, Christie MJ (1996) Opioid inhibition of rat periaqueductal grey neurones with identified projections to rostral ventromedial medulla in vitro. J Physiol 490 (Pt2):383–389.

Park C, Kim J-H, Yoon B-E, Choi E-J, Lee CJ, Shin H-S (2010) T-type channels control the opioidergic descending analgesia at the low threshold-spiking GABAergic neurons in the periaqueductal gray. PNAS 107:14857–14862.

Peirs C, Seal RP (2016) Neural circuits for pain: Recent advances and current views. Science 354:578–584.

Reiman A, Welty M, Solomon P (2017) Cannabis as a Substitute for Opioid-Based Pain Medication: Patient Self-Report. Cannabis Cannabinoid Res 2:160–166.

Samineni VK, Grajales-Reyes JG, Copits BA, O'Brien DE, Trigg SL, Gomez AM, Bruchas MR, Gereau RW IV (2017) Divergent Modulation of Nociception by Glutamatergic and GABAergic Neuronal Subpopulations in the Periaqueductal Gray. eNeuro 4:ENEURO.0129–16.2017–13.

Sturgeon JA, Khan J, Hah JM, Hilmoe H, Hong J, Ware MA, Mackey SC (2020) Clinical Profiles of Concurrent Cannabis Use in Chronic Pain: A CHOIR Study. Pain Med 21:3172–3179.

Suter BA, O'Connor T, Iyer V, Petreanu LT, Hooks BM, Kiritani T, Svoboda K, Shepherd GMG (2010) Ephus: multipurpose data acquisition software for neuroscience experiments. Front Neural Circuits 4:100.

Tonsfeldt KJ, Suchland KL, Beeson KA, Lowe JD, Li M-H, Ingram SL (2016) Sex Differences in GABAA Signaling in the Periaqueductal Gray Induced by Persistent Inflammation. J Neurosci 36:1669–1681.

Tracey I, Mantyh PW (2007) The cerebral signature for pain perception and its modulation. Neuron 55:377–391.

Trivers KF, Gentzke AS, Phillips E, Tynan M, Marynak KL, Schauer GL (2019) Substances used in electronic vapor products among adults in the United States, 2017. Addict Behav Rep 10:100222.

Vaughan CW, Bagley EE, Drew GM, Schuller A, Pintar JE, Hack SP, Christie MJ (2003) Cellular actions of opioids on periaqueductal grey neurons from C57B16/J mice and mutant mice lacking MOR-1. Br J Pharmacol 139:362–367.

Vaughan CW, Ingram SL, Connor MA, Christie MJ (1997) How opioids inhibit GABA-mediated neurotransmission. Nature 390:611–614.

Wiley JL, Taylor SI, Marusich JA (2021) Δ9-Tetrahydrocannabinol discrimination: Effects of route of administration in rats. Drug Alcohol Depend 225:108827.

Wilson AR, Maher L, Morgan MM (2008) Repeated cannabinoid injections into the rat periaqueductal gray enhance subsequent morphine antinociception. Neuropharmacology 55:1219–1225.

Wilson TD, Valdivia S, Khan A, Ahn H-S, Adke AP, Martinez Gonzalez S, Sugimura YK, Carrasquillo Y (2019) Dual and Opposing Functions of the Central Amygdala in the Modulation of Pain. Cell Rep 29:332–346.e335.

Wilson-Poe AR, Morgan MM, Aicher SA, Hegarty DM (2012) Distribution of CB1 cannabinoid receptors and their relationship with mu-opioid receptors in the rat periaqueductal gray. Neuroscience 213:191–200.

Wilson-Poe AR, Pocius E, Herschbach M, Morgan MM (2013) The periaqueductal gray contributes to bidirectional enhancement of antinociception between morphine and cannabinoids. Pharmacol Biochem Behav 103:444–449.

Woodhams SG, Chapman V, Finn DP, Hohmann AG, Neugebauer V (2017) The cannabinoid system and pain. Neuropharmacology 124:105–120.

Woodruff AR, Sah P (2007) Networks of parvalbumin-positive interneurons in the basolateral amygdala. J Neurosci 27:553–563.

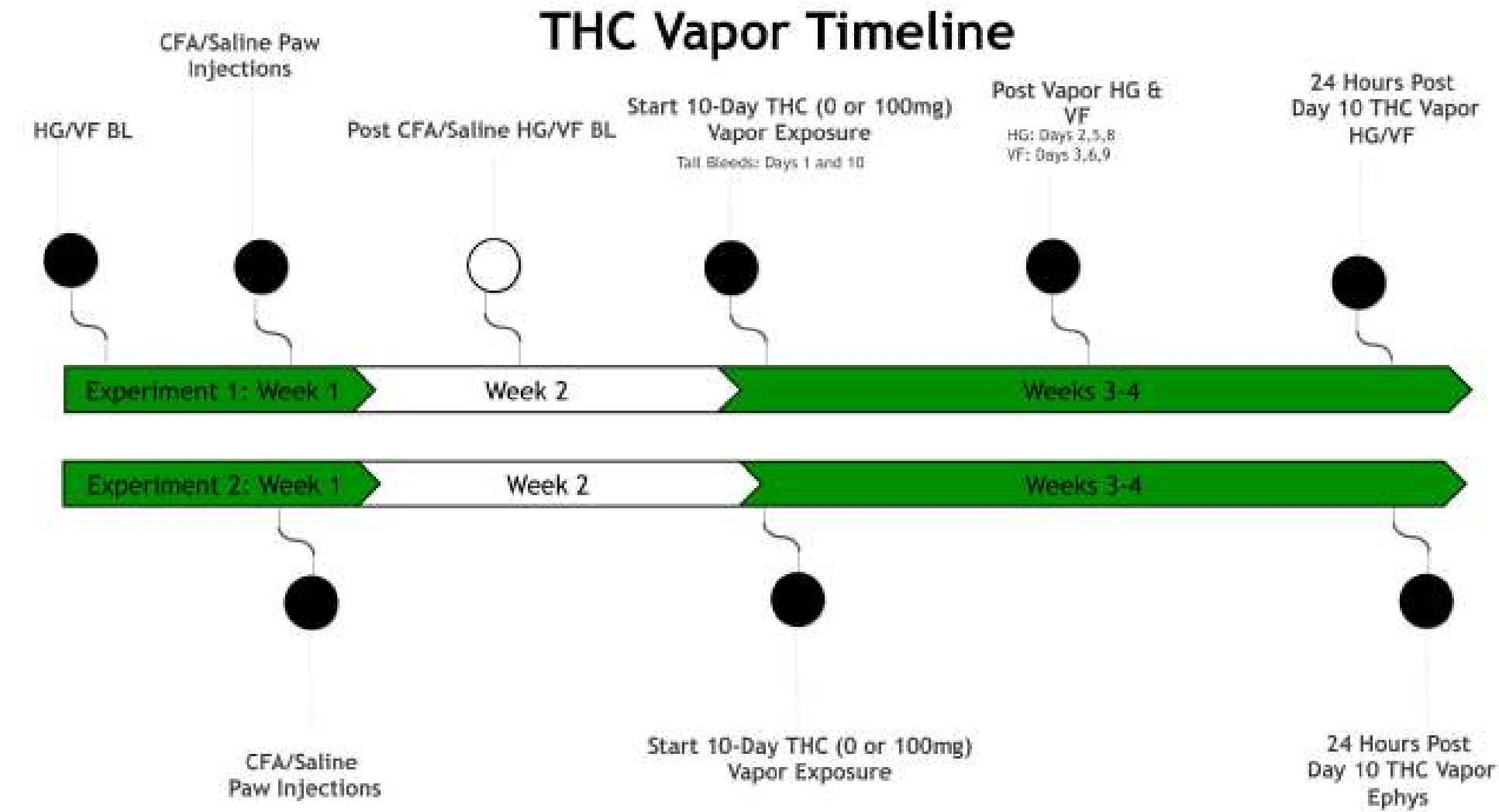

Figure 1. Kelley et al.

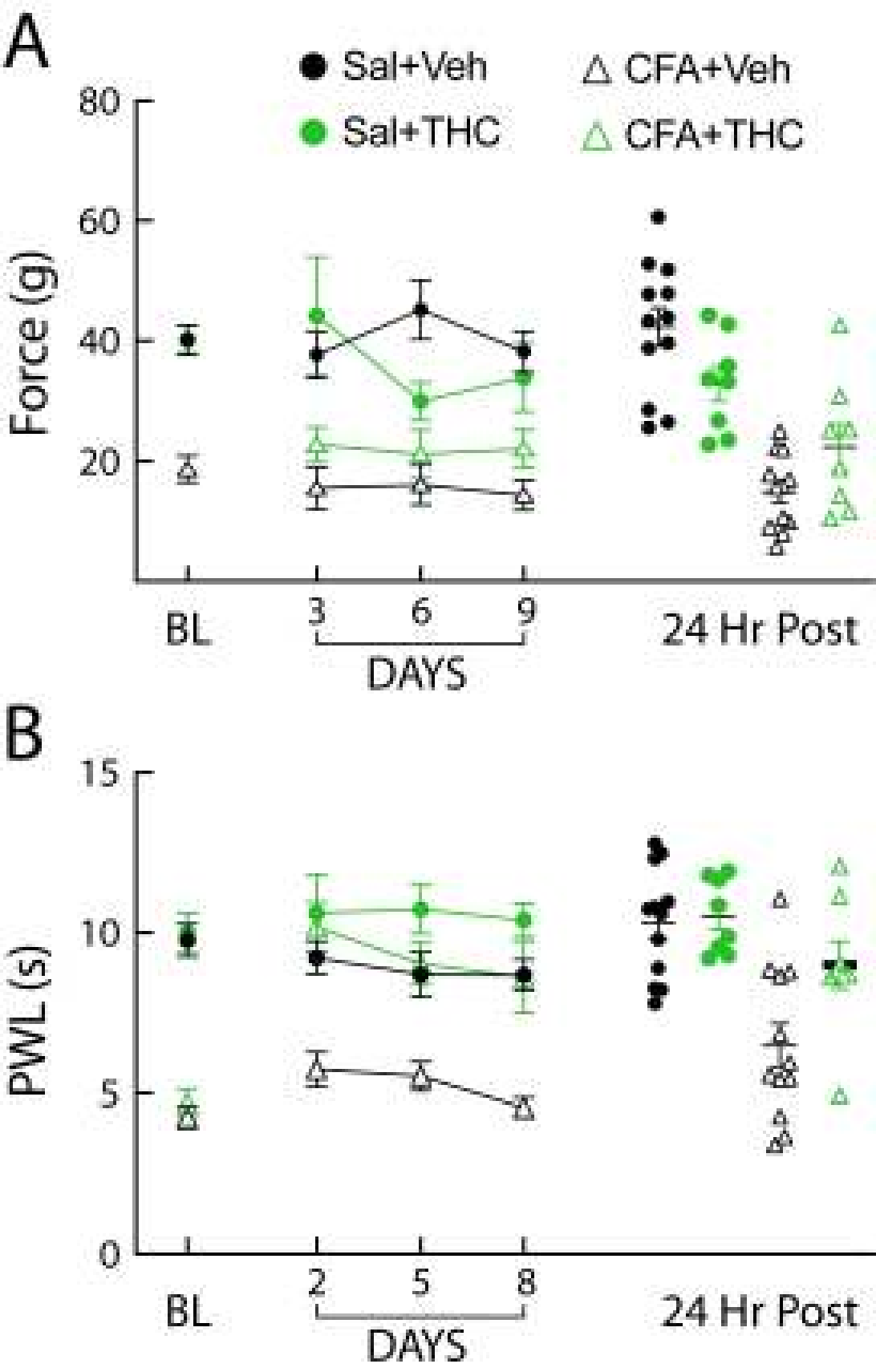

Figure 2. Kelley et al.

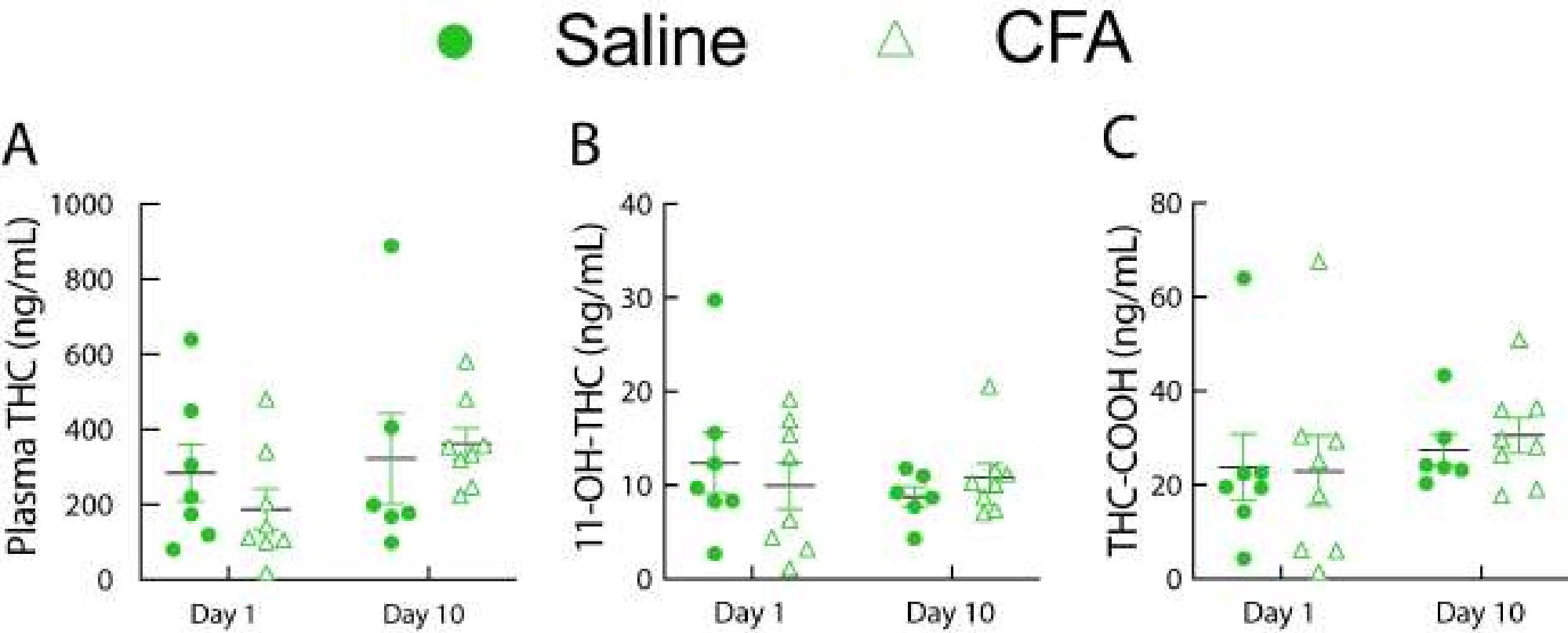

Figure 3. Kelley et al.

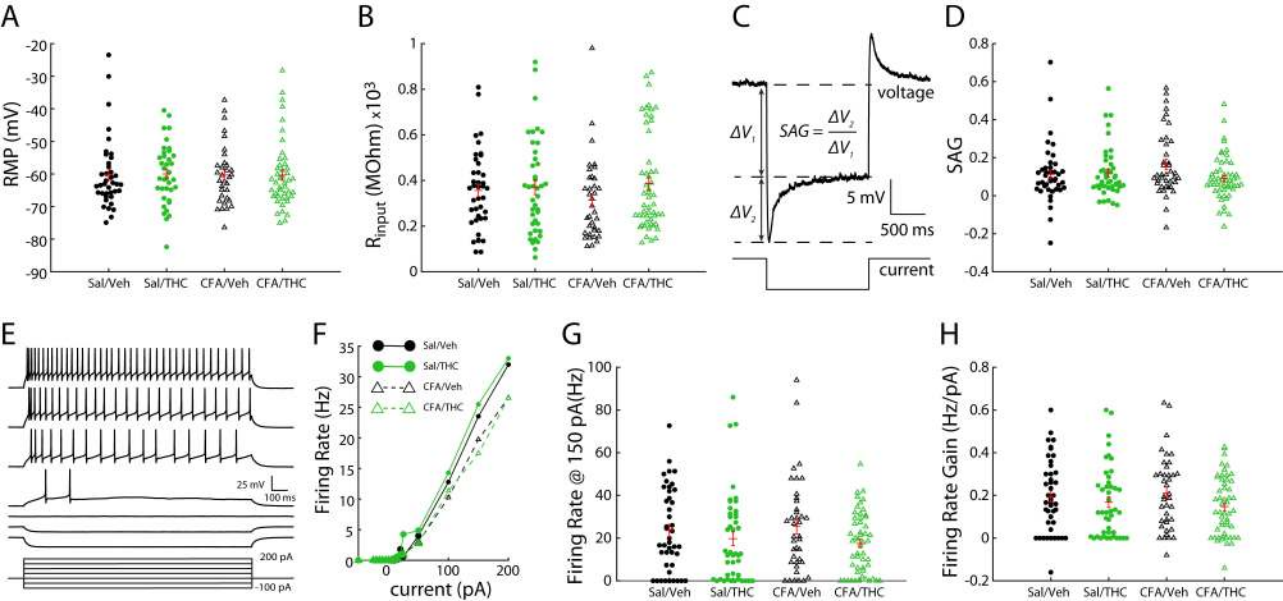

Figure 4. Kelley et al.

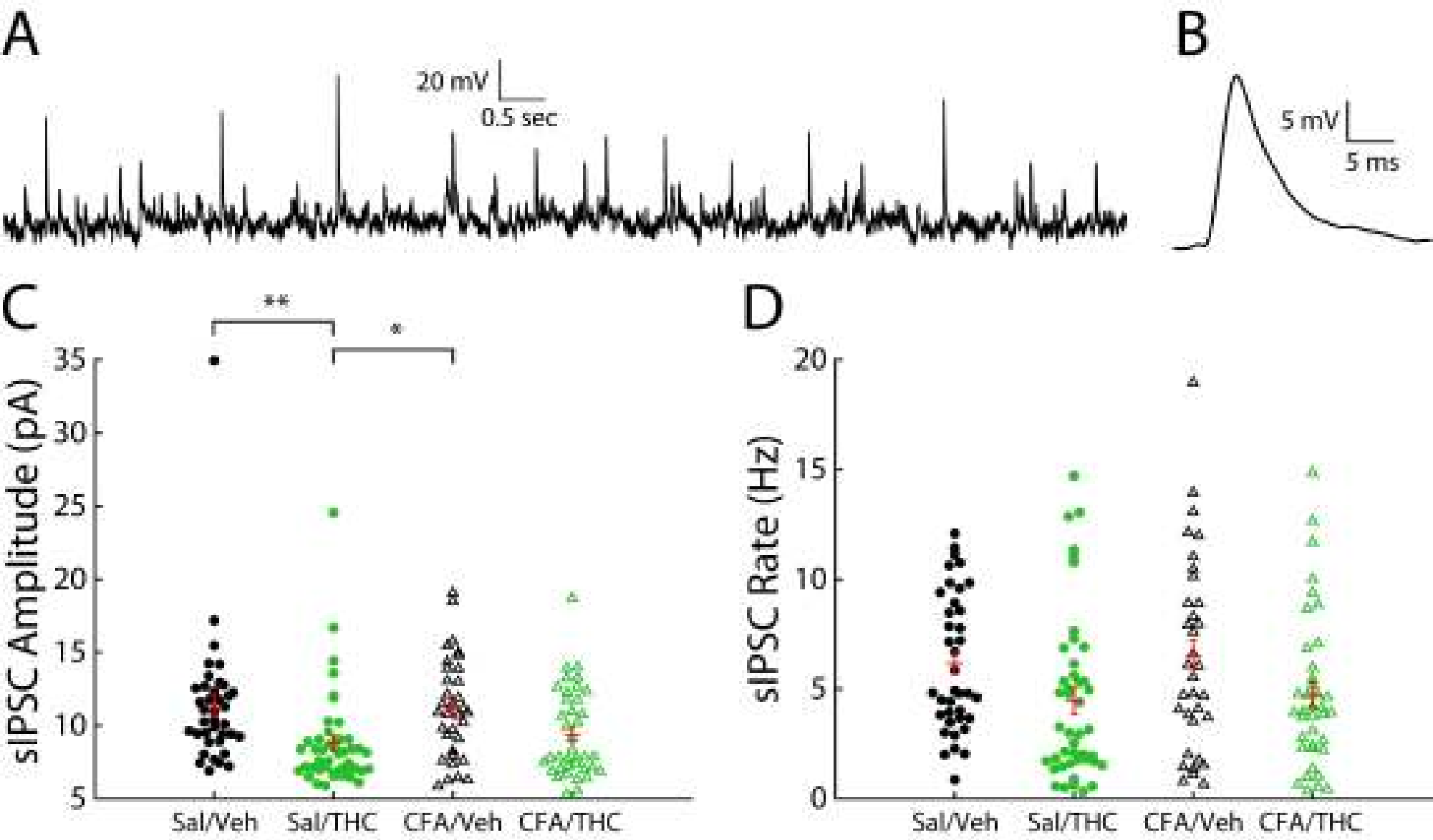

Figure 5. Kelley et al.

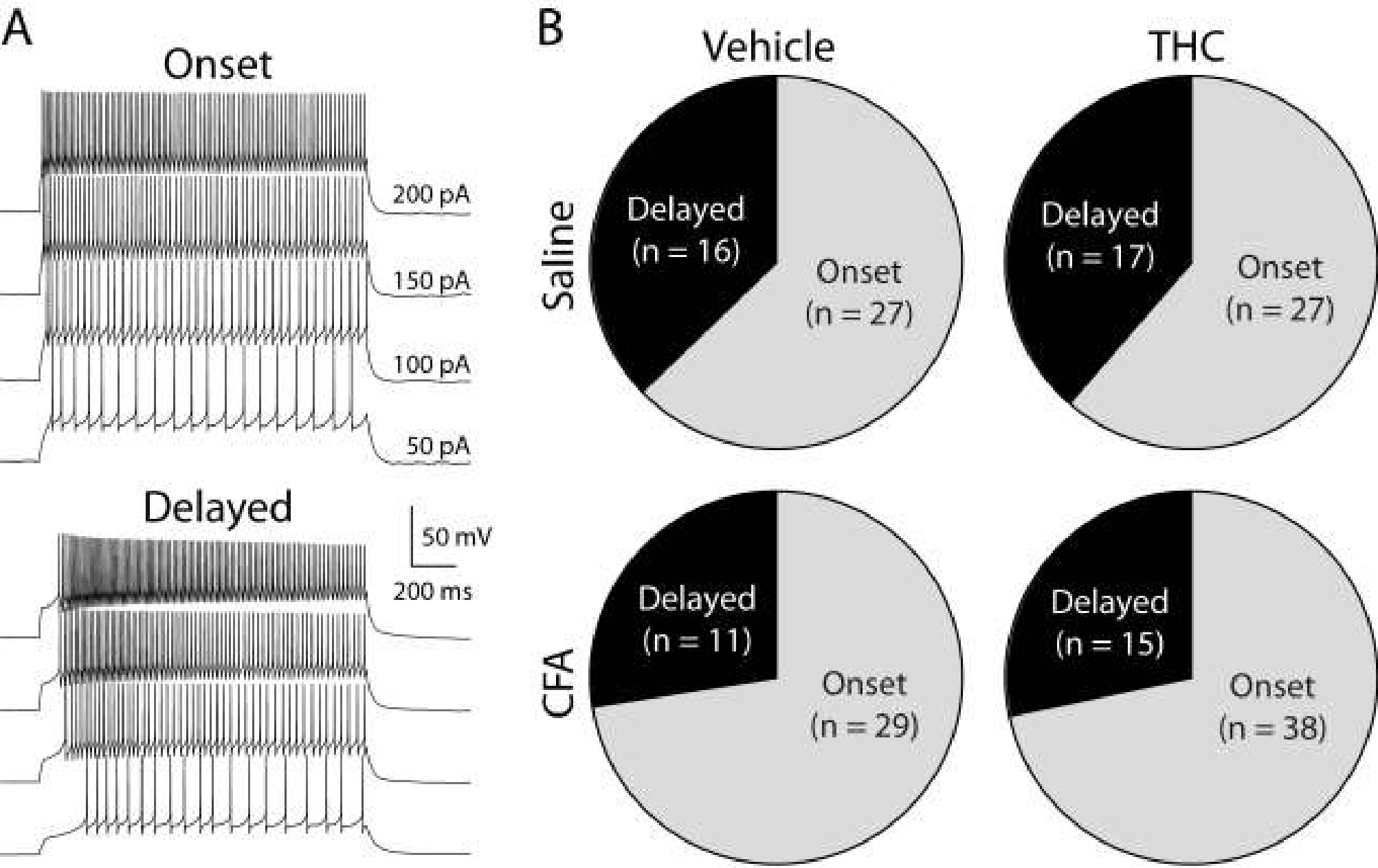

Figure 6. Kelley et al.

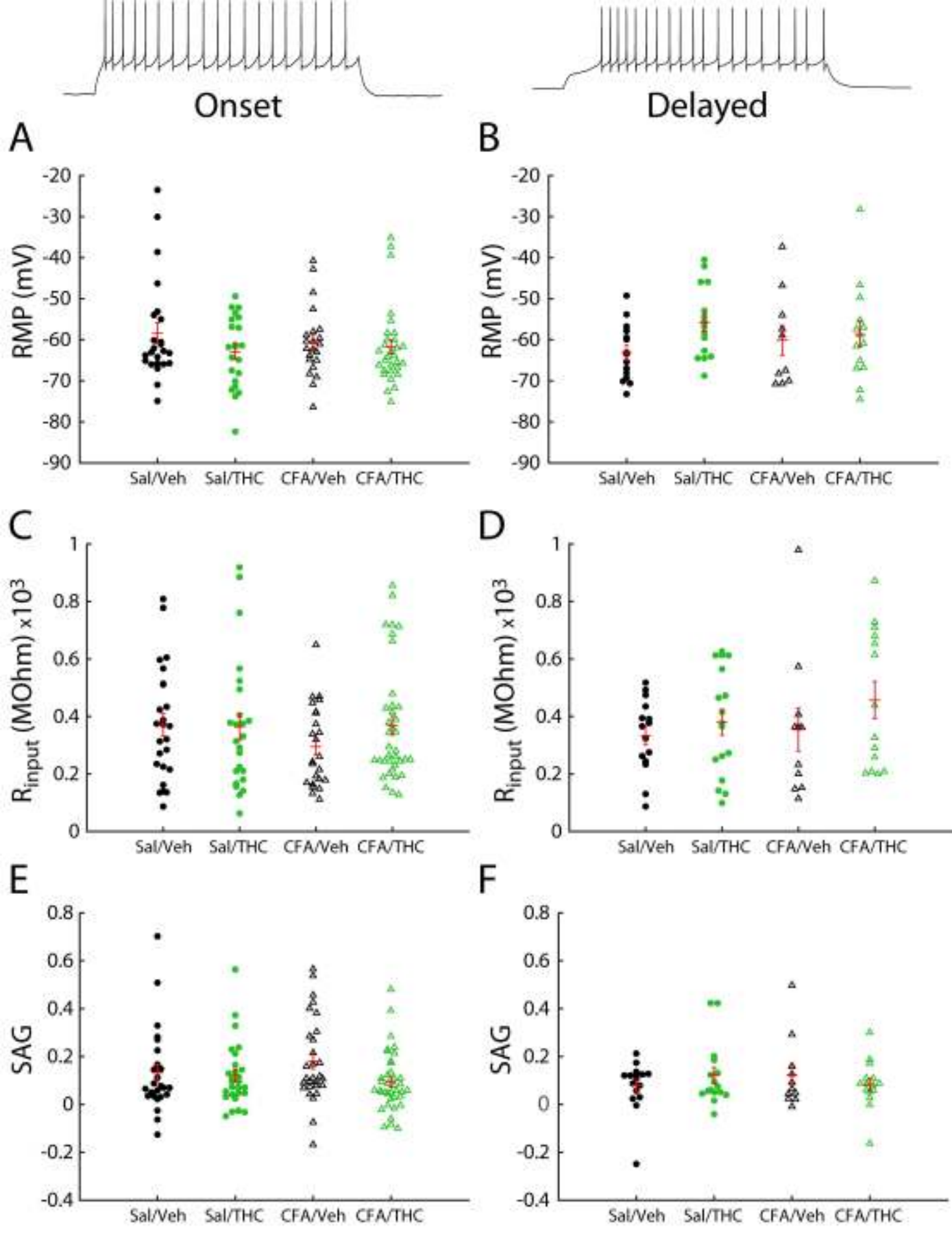

Figure 7. Kelley et al.

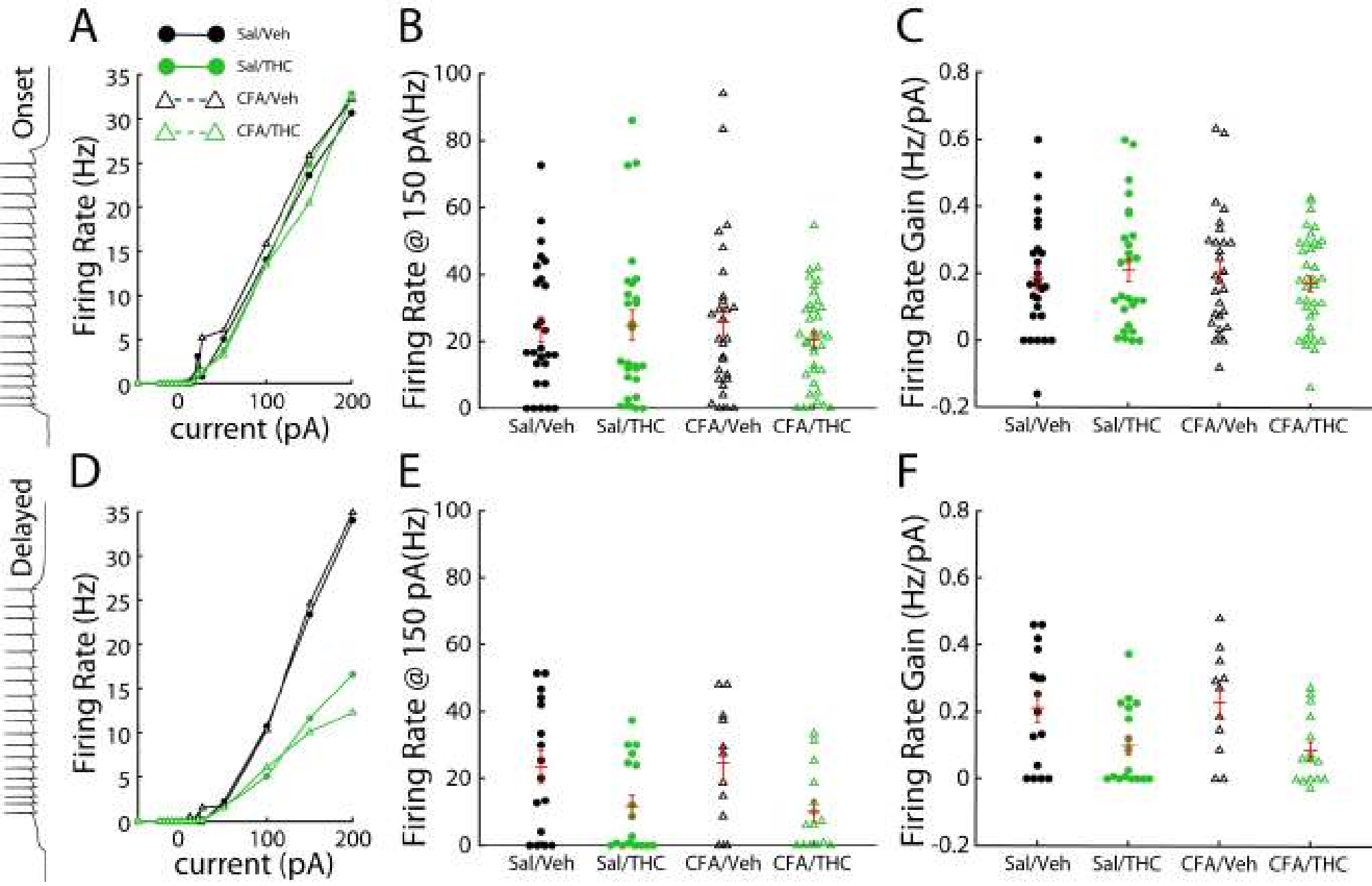

Figure 8. Kelley et al.

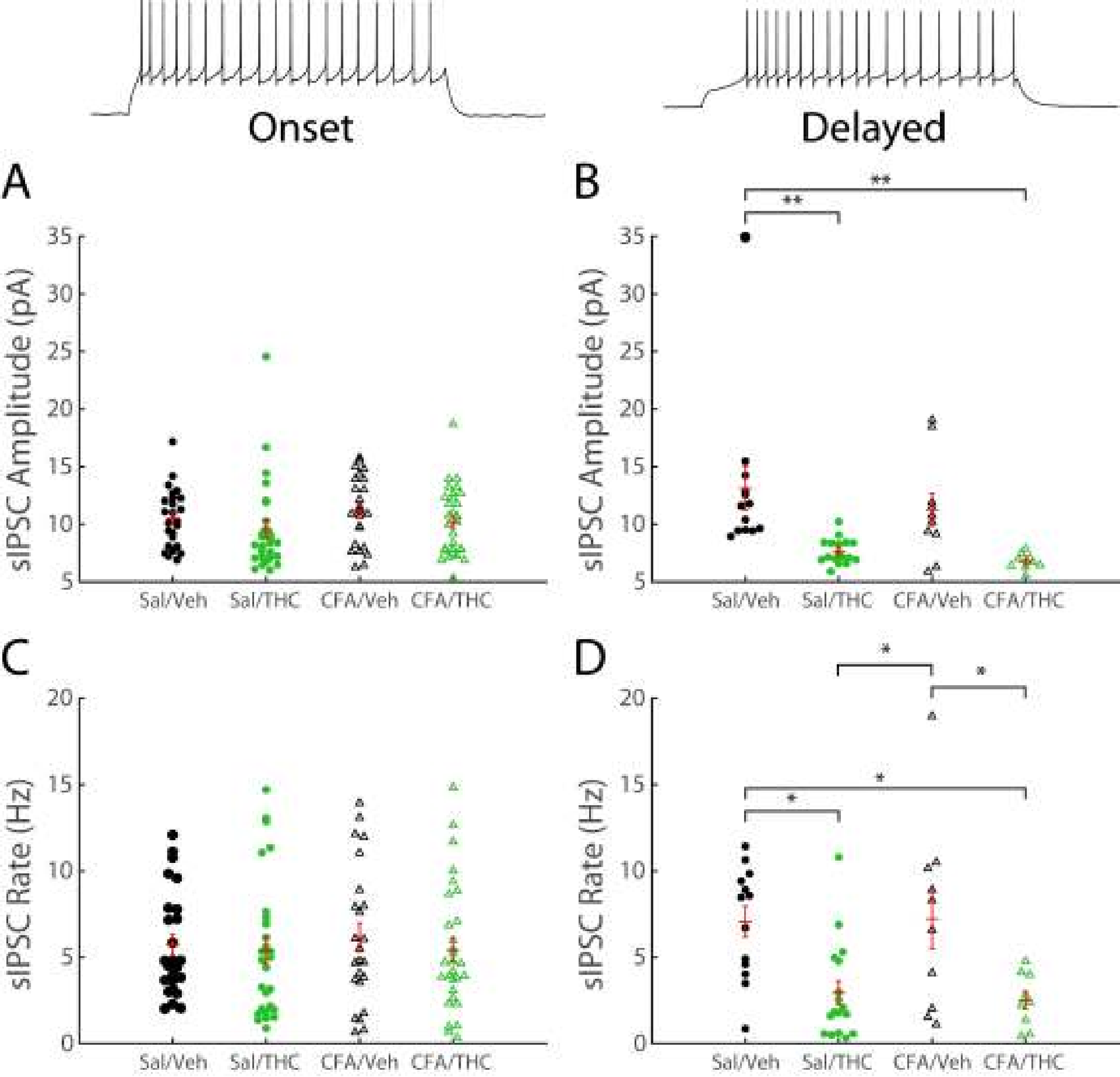

Figure 9. Kelley et al.

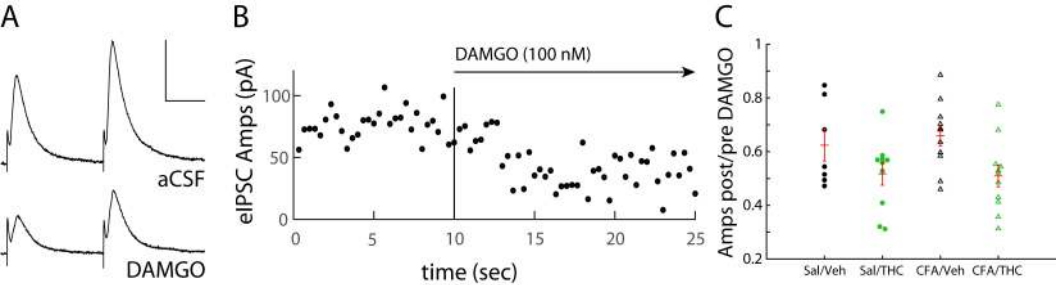

Figure 10. Kelley et al.